

Yukawa enhancement of Z -mediated New Physics in $\Delta S = 2$ and $\Delta B = 2$ Processes

Christoph Bobeth,^{1,2,4} Andrzej J. Buras,^{1,2} Alejandro Celis,³ Martin Jung⁴

¹TUM Institute for Advanced Study, Lichtenbergstr. 2a, D-85748 Garching, Germany

²Physik Department, TU München, James-Frank-Straße, D-85748 Garching, Germany

³Ludwig-Maximilians-Universität München, Fakultät für Physik,
Arnold Sommerfeld Center for Theoretical Physics, 80333 München, Germany

⁴Excellence Cluster Universe, Technische Universität München, Boltzmannstr. 2, D-85748
Garching, Germany

Abstract

We discuss Yukawa-enhanced contributions from Z -mediated new physics to down-type quark $\Delta F = 2$ processes in the framework of the standard model gauge-invariant effective theory (SMEFT). Besides the renormalization group (RG) mixing of the Z -mediating $\psi^2 H^2 D$ operators into $\Delta F = 2$ operators, we include at the electroweak scale one-loop (NLO) matching corrections consistently, necessary for the removal of the matching scale dependence. We point out that the right-handed Z -mediated interactions generate through Yukawa RG mixing $\Delta F = 2$ left-right operators, which are further enhanced through QCD RG effects and chirally enhanced hadronic matrix elements. We investigate the impact of these new effects on the known correlations between $\Delta F = 2$ and $\Delta F = 1$ transitions in the SMEFT framework and point out qualitative differences to previous parameterizations of Z -mediated new physics that arise for the left-handed case. We illustrate how specific models fit into our model-independent framework by using four models with vector-like quarks. We carry out model-independent analyses of scenarios with purely left-handed and purely right-handed new-physics Z couplings for each of the three sectors $s \rightarrow d$, $b \rightarrow s$ and $b \rightarrow d$. Specifically we discuss the correlations between ε'/ε , ε_K , $K_L \rightarrow \mu^+ \mu^-$, $K^+ \rightarrow \pi^+ \nu \bar{\nu}$ and $K_L \rightarrow \pi^0 \nu \bar{\nu}$ in the Kaon sector, and ϕ_s , $B_s \rightarrow \mu^+ \mu^-$ and $B \rightarrow K^{(*)}(\mu^+ \mu^-, \nu \bar{\nu})$ in the $b \rightarrow s$ sector and $B_d \rightarrow \mu^+ \mu^-$ in the $b \rightarrow d$ sector.

Contents

1	Introduction	2
2	SMEFT, $\Delta F=2$-EFT and Tree-level Matching	5
2.1	SMEFT	5
2.2	Effective Hamiltonian for $\Delta F = 2$	8
2.3	$\Delta F = 2$ Tree-level matching	9
3	Leading RG Effects in SMEFT	9
4	NLO Contributions in SMEFT	11
4.1	$\Delta F = 2$ NLO matching	11
4.2	Numerical Impact of NLO Contributions	14
4.3	NLO Contributions in VLQ Models	16
5	Comparison with the Literature	17
6	Implications for Flavour Observables	21
6.1	Numerical impact on M_{12}	23
6.2	Semileptonic $\Delta F = 1$ Processes	24
6.3	Correlations between $\Delta F = 2$ and $\Delta F = 1$ Processes	26
7	Summary and Conclusions	32
A	SMEFT	34
	References	36

1 Introduction

In the Standard Model (SM) tree-level flavour-changing (FC) couplings of the Z boson to quarks are forbidden by the Glashow-Iliopoulos-Maiani (GIM) mechanism [1]. At one-loop level the GIM mechanism is broken by the disparity of quark masses and such couplings are generated, for instance through the so-called Z -penguin diagrams. These play an important role specifically in rare K and $B_{s,d}$ decays ($\Delta F = 1$) in which the GIM mechanism is strongly broken because of the large top-quark mass. However, the related one-loop function $C(x_t)$ ($x_t = m_t^2/M_W^2$), one of the Inami-Lim functions [2], is gauge dependent and additional diagrams have to be included to cancel this gauge dependence. Only the resulting gauge-independent one-loop functions have physical meaning and consequently enter formulae for various rare decay observables [3], see [4] for a recent review.

In models beyond the SM (BSM) FC quark couplings of the Z can be present already at tree-level and hence contribute to rare K and $B_{s,d}$ decays as well as neutral meson mixing, that is, $\Delta F = 2$ processes. The relative size of these contributions can be very large, given the loop- and GIM-suppression present in the SM. Such scenarios can model-independently be treated in an effective theory invariant under the SM gauge group $G_{\text{SM}} = \text{SU}(3)_c \otimes \text{SU}(2)_L \otimes \text{U}(1)_Y$ (SMEFT) [5] if the new physics (NP) responsible for these couplings is weakly coupled, can be decoupled at some high scale $\mu_\Lambda \gg \mu_{\text{ew}}$, much larger than the scale μ_{ew} of electroweak symmetry breaking (EWSB), and no additional degrees of freedom are present besides the ones of the SM. FC quark couplings of the Z are then given at leading order (dimension six) by four operators of the non-redundant “Warsaw” basis [6]. Only three of these are relevant for down-quark $\Delta F = 1, 2$ flavour-changing neutral current (FCNC) phenomenology: two operators with a left-handed (LH) quark current, $\mathcal{O}_{Hq}^{(1,3)}$, and one with a right-handed (RH) quark current, \mathcal{O}_{Hd} . They belong to the class $\psi^2 H^2 D$ of operators with two fermion fields, two Higgs-doublet fields and one covariant derivative. We do not consider the fourth operator \mathcal{O}_{Hu} of this class which is relevant for up-quark processes, only. Operators of the class $\psi^2 H X$ of dipole operators, where X denotes the field strength tensors of G_{SM} , are suppressed by an additional factor of a light fermion mass for the processes considered below and hence also neglected.¹

The importance of Z -mediated FCNC processes has increased recently in view of the absence of direct NP signals at the LHC and given that the neutral Z is particularly suited to be a messenger of possible NP even at scales far beyond the reach of the LHC, see [8–11] for recent analyses. Here we analyze Z -mediated NP in the framework of SMEFT. The analysis yields several surprises concerning down-quark $\Delta F = 2$ processes, which to our knowledge have not been noticed so far in the literature:

1. In the presence of right-handed FC Z couplings, *i.e.* $\mathcal{C}_{Hd} \neq 0$ for a FC transition, inspection of the renormalization group (RG) equations due to Yukawa couplings in [12] yields that at μ_{ew} the left-right $\Delta F = 2$ operators $\mathcal{O}_{\text{LR},1}^{ij}$ in (19) are generated and are enhanced by the large leading logarithm $\ln \mu_\Lambda/\mu_{\text{ew}}$. Such operators are known to provide very important contributions to $\Delta F = 2$ observables because of their enhanced hadronic matrix elements and an additional enhancement from QCD RG effects below μ_{ew} , in particular in the K -meson system. As a result *these*

¹Furthermore, these operators are generated only at loop level in weakly coupled gauge theories [7].

operators – and not O_{VRR}^{ij} in (18), as used in [8–10] – dominate $\Delta F = 2$ processes. The results in [12] allow the calculation of this dominant contribution including only leading logarithms.

2. Because of the usual scale ambiguity present at leading order (LO) we calculate the next-to-leading order (NLO) matching corrections of \mathcal{O}_{Hd} to $\Delta F = 2$ processes at μ_{ew} within SMEFT. One NLO contribution is obtained by replacing the flavour-diagonal lepton vertex in the SM Z -penguin diagram by $[\mathcal{C}_{Hd}]_{ij}$ (see Fig. 1a), which again generates the operator $O_{\text{LR},1}^{ij}$ simply because the flavour-changing part of the SM penguin diagram is LH. In fact this contribution has been recently pointed out in [11] and used for phenomenology. Unfortunately, such contributions are by themselves gauge dependent, simply because the function $C(x_t)$ present in the SM vertex is gauge dependent. Hence, while the observation made in [11] is important, the analysis of these new contributions presented there is incomplete.² In the present paper we calculate the missing contributions using SMEFT, obtaining a new gauge-independent function. This contribution itself is by about a factor of two smaller than the one found in [11] (with the same sign), however, the LO contribution is not only more important due to the large logarithm $\ln \mu_{\Lambda}/\mu_{\text{ew}}$, but has also opposite sign, allowing to remove the LO scale dependence. The total new contribution that includes LO and NLO terms in SMEFT is larger and has opposite sign to the one found in [11]. Moreover being strongly enhanced with respect to the contributions considered in [8–10], it has a very large impact on the phenomenology; in particular the correlations between $\Delta F = 2$ and $\Delta F = 1$ observables are drastically changed.
3. The situation for LH FC Z couplings is different from the RH case both qualitatively and quantitatively: inspecting again the RG equations in [12] we find that the two operators $\mathcal{O}_{Hq}^{(1)}$ and $\mathcal{O}_{Hq}^{(3)}$ in SMEFT generate only the $\Delta F = 2$ -operator O_{VLL} dominant already in the SM, which is the same as generated by the contributions considered in [8]. The resulting NP effects in $\Delta F = 2$ transitions are then much smaller than in the RH case, because no LR operators are present. Importantly, the correlations between $\Delta F = 1$ and $\Delta F = 2$ processes are changed dramatically: while $\Delta F = 1$ transition amplitudes are proportional to the sum $\mathcal{C}_{Hq}^{(1)} + \mathcal{C}_{Hq}^{(3)}$, the leading RG contribution to $\Delta F = 2$ processes is proportional to the difference of these couplings. Correlations between $\Delta F = 1$ and $\Delta F = 2$ processes are hence only present in specific models. This is in stark contrast to the contributions considered in [8] and also used in [11], where the same couplings enter both classes of processes.³ Of course correlations remain in each sector separately, since both are governed by two parameters, only. Interestingly this allows to access *both* coefficients *separately* from $\Delta F = 2$ and $\Delta F = 1$ observables, which did not seem possible before. In models where $\Delta F = 2$ and $\Delta F = 1$ observables are correlated, the constraints

²After the appearance of our paper the authors of [11] included the remaining contributions obtaining a gauge independent NLO correction to \mathcal{C}_{Hd} which agrees with ours. Unfortunately they did not include RG Yukawa effects above μ_{ew} , discussed in point 1. above, so that their result depends very strongly on μ_{ew} as we will demonstrate in Section 5.

³In particular in [11] the choice $\mathcal{C}_{Hq}^{(3)} = 0$ has been made, which can only be true at a single renormalization scale.

become weaker, allowing for larger NP effects in rare decays.

4. Also for the operators $\mathcal{O}_{Hq}^{(1,3)}$ the NLO contributions to $\Delta F = 2$ transitions corresponding to the replacement of the flavour-diagonal lepton vertex in the SM Z -penguin diagram Fig. 1a by $\mathcal{C}_{Hq}^{(1,3)}$ are gauge dependent. We include the remaining contributions to remove this gauge dependence and find a second gauge-independent function. Since the NLO contributions are different for $\mathcal{C}_{Hq}^{(1)}$ and $\mathcal{C}_{Hq}^{(3)}$, it is not just their difference contributing to O_{VLL} anymore, but also their sum. In fact, $SU(2)_L$ gauge invariance in SMEFT imposes relations between down-type and up-type quark FCNCs that are governed by these operators, for example between $B_{d,s}$ -mixing and $t \rightarrow (u, c)$ processes.
5. At NLO also new gauge-independent contributions are generated which are unrelated to tree-level Z exchanges and only proportional to $\mathcal{C}_{Hq}^{(3)}$, analogous to the usual box diagrams with W^\pm and quark exchanges. They turn out to be important for gauge-independence and depend not only on the coefficients for the quark transition under consideration, but also on additional ones corresponding to the possible intermediate quarks in the box diagrams.

It should be stressed in this context that the contributions to $\Delta F = 2$ transitions from FC quark couplings of the Z could be less relevant in NP scenarios with other sources of $\Delta F = 2$ contributions. Most importantly, $\Delta F = 2$ operators could receive a direct contribution at tree-level at the scale μ_Λ , but also in models where this does not happen Z contributions could be subdominant. Examples are models in which the only new particles are vector-like quarks (VLQs), where box diagrams with VLQ and Higgs exchanges generate $\Delta F = 2$ operators at one-loop level [13, 14], which were found in these papers to be larger than the Z contributions at tree-level. However, in [13] and in the first version of our analysis in [14] the effects listed above have not been included. As we will see below, for right-handed FC Z couplings these box contributions are dwarfed by the LR operator contributions mentioned at the beginning of our list in Kaon mixing, whereas in B -mixing they are comparable.

The outline of our paper is as follows: In Section 2 we establish notation, recall the parts of SMEFT and the effective Hamiltonian for $\Delta F = 2$ transitions most important for our work, and summarise the tree-level matching between the two at μ_{ew} . In Section 3 we summarise the results of the RG evolution in SMEFT. In Section 4 we present the results of the NLO contributions to the matching at μ_{ew} with some details relegated to Appendix A. The main outcome of this section are gauge-independent functions $H_1(x_t, \mu_{ew})$ and $H_2(x_t, \mu_{ew})$ that are analogous to the $\Delta F = 1$ loop functions of [3]. Their dependence on the electroweak scale μ_{ew} cancels the scale dependence of the Wilson coefficients resulting from the RG evolution. We illustrate the size of NLO effects model-independently considering LH and RH couplings individually and in the context of models with vector-like quarks (VLQs) using the results from [13–15]. In Section 5 we compare the framework of SMEFT used here with simplified models of FC quark couplings of the Z considered previously in [8–11], stressing significant limitations of these models as far as FCNCs mediated by Z exchanges are concerned.⁴ In particular we compare our results to those

⁴Our critical analysis does not apply to Z' models considered in these papers.

of [11] who included some of the NLO contributions considered by us in the framework of simplified models, reaching conclusions rather different from our findings. In Section 6 we study model-independently the impact of the presence of $\psi^2 H^2 D$ operators on the correlation between $\Delta F = 1$ and $\Delta F = 2$ processes, like the $s \rightarrow d$ transitions ε'/ε , ε_K , $K^+ \rightarrow \pi^+ \nu \bar{\nu}$ and $K_L \rightarrow \pi^0 \nu \bar{\nu}$ and the $b \rightarrow d, s$ transitions $\Delta m_{d,s}$, $B_{d,s} \rightarrow \mu^+ \mu^-$ or $B \rightarrow K^{(*)}(\mu^+ \mu^-, \nu \bar{\nu})$. We conclude in Section 7.

2 SMEFT, $\Delta F = 2$ -EFT and Tree-level Matching

Throughout we assume that NP interactions have been integrated out at some scale $\mu_\Lambda \gg \mu_{\text{ew}}$, giving rise to the SMEFT framework. The field content of the SMEFT-Lagrangian are the SM fields and the interactions are invariant under the SM gauge group G_{SM} ; the corresponding Lagrangian can be written as

$$\mathcal{L}_{\text{SMEFT}} = \mathcal{L}_{\text{dim-4}} + \sum_a \mathcal{C}_a \mathcal{O}_a. \quad (1)$$

Here $\mathcal{L}_{\text{dim-4}}$ coincides with the SM Lagrangian and a non-redundant set of operators of dimension six (dim-6), \mathcal{O}_a , has been classified in [6]. The anomalous dimensions (ADM) necessary for the RG evolution from μ_Λ to μ_{ew} of the SM couplings and the Wilson coefficients \mathcal{C}_a are known at one-loop [12, 16, 17]. Given some initial coefficients $\mathcal{C}_a(\mu_\Lambda)$, they can be evolved down to μ_{ew} , thereby resumming leading logarithmic (LLA) effects due to the quartic Higgs, gauge and Yukawa couplings into $\mathcal{C}_a(\mu_{\text{ew}})$. Far above μ_{ew} it is convenient to work in the unbroken $SU(2)_L \otimes U(1)_Y$ phase, however close to μ_{ew} EWSB is taking place and it is more convenient to transform gauge bosons and fermions from the weak to their mass eigenstates.

For the purpose of down-quark $\Delta F = 1, 2$ phenomenology a second decoupling of heavy SM degrees of freedom (W^\pm, Z, H, t) takes place at the electroweak scale μ_{ew} . It gives rise to the $\Delta F = 1, 2$ effective Hamiltonians (EFT) with the gauge symmetry $SU(3)_c \otimes U(1)_{\text{em}}$ and number of active quark flavours $N_f = 5, 4, 3$ when going below the b - and c -quark thresholds [18].

We use the following notation for Wilson coefficients and operators in the corresponding effective theories:

$$\begin{aligned} \text{SMEFT: } \mathcal{L}_{\text{SMEFT}} &\sim \mathcal{C}_a \mathcal{O}_a, \\ \Delta F = 2\text{-EFT: } \mathcal{H}_{\Delta F=2} &\sim C_a \mathcal{O}_a. \end{aligned} \quad (2)$$

Note the use of the Lagrangian \mathcal{L} for SMEFT, but the Hamiltonian \mathcal{H} for the $\Delta F = 2$ -EFT.⁵

2.1 SMEFT

In this work we are concerned with operators that induce FC quark couplings of the Z and their impact on the four-fermion (ψ^4) operators that mediate $\Delta F = 2$ down-type

⁵Note the relative sign $\mathcal{L} = -\mathcal{H}$.

quark transitions. The relevant operators in the quark sector belong to the class $\psi^2 H^2 D$. The ones with LH quark currents are ⁶

$$\mathcal{O}_{Hq}^{(1)} = (H^\dagger i \overleftrightarrow{\mathcal{D}}_\mu H) [\bar{q}_L^i \gamma^\mu q_L^j], \quad \mathcal{O}_{Hq}^{(3)} = (H^\dagger i \overleftrightarrow{\mathcal{D}}_\mu^a H) [\bar{q}_L^i \sigma^a \gamma^\mu q_L^j], \quad (3)$$

including also modified LH W^\pm couplings. The ones with RH quark currents are

$$\mathcal{O}_{Hd} = (H^\dagger i \overleftrightarrow{\mathcal{D}}_\mu H) [\bar{d}_R^i \gamma^\mu d_R^j], \quad \mathcal{O}_{Hu} = (H^\dagger i \overleftrightarrow{\mathcal{D}}_\mu H) [\bar{u}_R^i \gamma^\mu u_R^j]. \quad (4)$$

Finally there is one operator with charged RH quark currents:

$$\mathcal{O}_{Hud} = (\tilde{H}^\dagger i \mathcal{D}_\mu H) [\bar{u}_R^i \gamma^\mu d_R^j]. \quad (5)$$

Here $\tilde{H} \equiv i\sigma_2 H^*$ and more details on conventions are given in Appendix A. The complex-valued coefficients of these operators are denoted by

$$[\mathcal{C}_{Hq}^{(1)}]_{ij}, \quad [\mathcal{C}_{Hq}^{(3)}]_{ij}, \quad [\mathcal{C}_{Hd}]_{ij}, \quad [\mathcal{C}_{Hu}]_{ij}, \quad [\mathcal{C}_{Hud}]_{ij}, \quad (6)$$

where the indices $ij = 1, 2, 3$ denote the different generations of up- and down-type quarks.

After EWSB, the transition from a weak to the mass eigenbasis takes place for gauge and quark fields. The quark fields are rotated by 3×3 unitary rotations in flavour space

$$\psi_L \rightarrow V_L^\psi \psi_L, \quad \psi_R \rightarrow V_R^\psi \psi_R, \quad (7)$$

for $\psi = u, d$, such that

$$V_L^{\psi\dagger} m_\psi V_R^\psi = m_\psi^{\text{diag}}, \quad V \equiv (V_L^u)^\dagger V_L^d, \quad (8)$$

with diagonal up- and down-quark mass matrices m_ψ^{diag} . The non-diagonal mass matrices m_ψ include the contributions of dim-6 operators. The quark-mixing matrix V is unitary, similar to the CKM matrix of the SM; however, in the presence of dim-6 contributions the numerical values are different from those obtained in usual SM CKM-fits. Throughout we will take the freedom to choose the weak basis such that down quarks are already mass eigenstates, which fixes $V_{L,R}^d = \mathbb{1}$, and assume without loss of generality $V_R^u = \mathbb{1}$, yielding $q_L = (V^\dagger u_L, d_L)^T$.

The $\psi^2 H^2 D$ operators lead to modifications of the couplings of quarks to the weak gauge bosons ($V = W^\pm, Z$ and $g_Z \equiv \sqrt{g_1^2 + g_2^2}$):

$$\begin{aligned} \mathcal{L}_{\psi\bar{\psi}V}^{\text{dim-6}} = & -\frac{g_Z}{2} v^2 Z_\mu \left(\left[V_L^{d\dagger} (\mathcal{C}_{Hq}^{(1)} + \mathcal{C}_{Hq}^{(3)}) V_L^d \right]_{ij} [\bar{d}_i \gamma^\mu P_L d_j] + \left[V_R^{d\dagger} \mathcal{C}_{Hd} V_R^d \right]_{ij} [\bar{d}_i \gamma^\mu P_R d_j] \right. \\ & \left. + \left[V_L^{u\dagger} (\mathcal{C}_{Hq}^{(1)} - \mathcal{C}_{Hq}^{(3)}) V_L^u \right]_{ij} [\bar{u}_i \gamma^\mu P_L u_j] + \left[V_R^{u\dagger} \mathcal{C}_{Hu} V_R^u \right]_{ij} [\bar{u}_i \gamma^\mu P_R u_j] \right) \\ & + \frac{g_2}{\sqrt{2}} v^2 \left(\left[V_L^{u\dagger} \mathcal{C}_{Hq}^{(3)} V_L^d \right]_{ij} [\bar{u}_i \gamma^\mu P_L d_j] W_\mu^+ + \left[V_R^{u\dagger} \frac{\mathcal{C}_{Hud}}{2} V_R^d \right]_{ij} [\bar{u}_i \gamma^\mu P_R d_j] W_\mu^+ + \text{h.c.} \right), \end{aligned} \quad (9)$$

⁶In order to simplify notations we suppress flavour indices on the operators.

where we display all rotation matrices for completeness. Note that in our notation fermion fields with an index for their handedness correspond to weak eigenstates, whereas mass eigenstates – like in this equation – do not carry this index. The values for v and the gauge couplings $g_{1,2}$ differ from the SM ones by dim-6 contributions. However, since the couplings in (9) are already at the level of dim-6, such corrections would count as dim-8 contributions, which is of higher order than considered here. From this equation it is apparent that our definition of the Wilson coefficients $[\mathcal{C}_a]_{ij}$ (at μ_{ew}) for our special choice of the weak quark basis – $V_{L,R}^d = \mathbb{1}$ and $V_R^u = \mathbb{1}$ – is particularly convenient for the study of down-type quark $\Delta F = 1, 2$ transitions, see also [19], because additional CKM factors appear only in couplings of operators involving left-handed up-type quarks. Thus the associated Wilson coefficients $\mathcal{C}_{Hq}^{(1,3)}$ enter down- *and* up-type-quark processes, leading to correlations between the affected processes that depend on the appearing CKM factors. As an example let us consider the top-quark FCNC coupling $t \rightarrow cZ$ ($i = c, j = t$),

$$\mathcal{L}_{t \rightarrow cZ}^{\text{dim-6}} \propto \sum_{k,l} V_{ck} [\mathcal{C}_{Hq}^{(1)} - \mathcal{C}_{Hq}^{(3)}]_{kl} V_{tl}^* \approx [\mathcal{C}_{Hq}^{(1)} - \mathcal{C}_{Hq}^{(3)}]_{sb} + \mathcal{O}(\lambda_C), \quad (10)$$

where we have neglected in the second step contributions suppressed by the Cabibbo angle λ_C and assumed that $V_{cs} \sim V_{tb} \sim \mathcal{O}(1)$ in SMEFT. Moreover, we have assumed that the Wilson coefficients themselves are all of the same size and hence do not upset the hierarchy of the CKM factors. In this case in fact B_s -mixing depends on above linear combination – see the result (30) – and hence is directly correlated to $t \rightarrow cZ$ FCNC decays. Under the same assumptions, also B_d and Kaon mixing are related to $t \rightarrow uZ$ and $c \rightarrow uZ$ FCNC decays, respectively.

We will omit \mathcal{O}_{Hu} and \mathcal{O}_{Hud} in the phenomenological part of our work,⁷ where we deal with down-type quark $\Delta F = 1, 2$ processes. The Wilson coefficients $\mathcal{C}_{Hq}^{(1,3)}$, \mathcal{C}_{Hd} (and \mathcal{C}_{Hu}) are complex-valued matrices in flavour space with a symmetric real part and antisymmetric imaginary part, such that each contains $6 + 3 = 9$ real degrees of freedom.

It is customary to parameterize FC quark couplings of the Z as [8]

$$\mathcal{L}_{\psi\bar{\psi}Z}^{\text{NP}} = Z_\mu \sum_{\psi=u,d} \bar{\psi}_i \gamma^\mu \left([\Delta_L^\psi]_{ij} P_L + [\Delta_R^\psi]_{ij} P_R \right) \psi_j. \quad (11)$$

This parameterization introduces also complex-valued couplings, whose relation to the dim-6 SMEFT tree-level contributions can be read off as

$$\begin{aligned} [\Delta_L^u]_{ij} &= -\frac{g_Z}{2} v^2 \left[\mathcal{C}_{Hq}^{(1)} - \mathcal{C}_{Hq}^{(3)} \right]_{ij}, & [\Delta_R^u]_{ij} &= -\frac{g_Z}{2} v^2 [\mathcal{C}_{Hu}]_{ij}, \\ [\Delta_L^d]_{ij} &= -\frac{g_Z}{2} v^2 \left[\mathcal{C}_{Hq}^{(1)} + \mathcal{C}_{Hq}^{(3)} \right]_{ij}, & [\Delta_R^d]_{ij} &= -\frac{g_Z}{2} v^2 [\mathcal{C}_{Hd}]_{ij}, \end{aligned} \quad (12)$$

in the special weak basis advocated before for the Wilson coefficients. We will comment in detail in Section 5 on the validity of this approach that does not incorporate the SM-gauge invariance and can only be justified when neglecting the Yukawa RG effects and hence adapted only at tree-level.

⁷This is mainly justified because their RG flow does not induce leading logarithmic contributions to down-type quark $\Delta F = 1, 2$ processes.

The ψ^4 operators that mediate $\Delta F = 2$ transitions are in SMEFT the $(\bar{L}L)(\bar{L}L)$ operators

$$[\mathcal{O}_{qq}^{(1)}]_{ijkl} = [\bar{q}_L^i \gamma_\mu q_L^j][\bar{q}_L^k \gamma^\mu q_L^l], \quad [\mathcal{O}_{qq}^{(3)}]_{ijkl} = [\bar{q}_L^i \gamma_\mu \sigma^a q_L^j][\bar{q}_L^k \gamma^\mu \sigma^a q_L^l], \quad (13)$$

the $(\bar{L}L)(\bar{R}R)$ operators

$$[\mathcal{O}_{qd}^{(1)}]_{ijkl} = [\bar{q}_L^i \gamma_\mu q_L^j][\bar{d}_R^k \gamma^\mu d_R^l], \quad [\mathcal{O}_{qd}^{(8)}]_{ijkl} = [\bar{q}_L^i \gamma_\mu T^A q_L^j][\bar{d}_R^k \gamma^\mu T^A d_R^l], \quad (14)$$

and the $(\bar{R}R)(\bar{R}R)$ operator

$$[\mathcal{O}_{dd}]_{ijkl} = [\bar{d}_R^i \gamma_\mu d_R^j][\bar{d}_R^k \gamma^\mu d_R^l], \quad (15)$$

with $kl = ij$ for $\Delta F = 2$ processes. The T^A denote $SU(3)_c$ colour generators.

2.2 Effective Hamiltonian for $\Delta F = 2$

The decoupling of heavy SM degrees of freedom at μ_{ew} gives rise to the $\Delta F = 2$ effective Hamiltonian [20, 21]

$$\mathcal{H}_{\Delta F=2}^{ij} = \mathcal{N}_{ij} \sum_a C_a^{ij} O_a^{ij} + \text{h.c.}, \quad (16)$$

where the normalisation factor and the CKM combinations are

$$\mathcal{N}_{ij} = \frac{G_F^2}{4\pi^2} M_W^2 (\lambda_t^{ij})^2, \quad \lambda_t^{ij} = V_{ti}^* V_{tj}, \quad (17)$$

with $ij = sd$ for kaon mixing and $ij = bd, bs$ for B_d and B_s mixing, respectively. The important operators for our discussion are in the operator basis of [21]

$$O_{\text{VLL}}^{ij} = [\bar{d}_i \gamma_\mu P_L d_j][\bar{d}_i \gamma^\mu P_L d_j], \quad O_{\text{VRR}}^{ij} = [\bar{d}_i \gamma_\mu P_R d_j][\bar{d}_i \gamma^\mu P_R d_j], \quad (18)$$

$$O_{\text{LR},1}^{ij} = [\bar{d}_i \gamma_\mu P_L d_j][\bar{d}_i \gamma^\mu P_R d_j], \quad O_{\text{LR},2}^{ij} = [\bar{d}_i P_L d_j][\bar{d}_i P_R d_j], \quad (19)$$

and the complete set can be found in [20, 21], where also the ADM matrices have been calculated up to NLO in QCD. We use these results in the QCD RG evolution from the electroweak scale μ_{ew} to low-energy scales.

In the SM only

$$C_{\text{VLL}}^{ij}(\mu_{\text{ew}})|_{\text{SM}} = S_0(x_t), \quad S_0(x) = \frac{x(4 - 11x + x^2)}{4(x-1)^2} + \frac{3x^3 \ln x}{2(x-1)^3} \quad (20)$$

is non-zero at the scale μ_{ew} .

2.3 $\Delta F = 2$ Tree-level matching

The SMEFT is matched to the $\Delta F = 2$ -EFT at μ_{ew} and at tree-level one finds the following modifications of the Wilson coefficients [19]:

$$\begin{aligned}\Delta C_{\text{VLL}}^{ij} &= -\mathcal{N}_{ij}^{-1} ([\mathcal{C}_{qq}^{(1)}]_{ijij} + [\mathcal{C}_{qq}^{(3)}]_{ijij}), & \Delta C_{\text{VRR}}^{ij} &= -\mathcal{N}_{ij}^{-1} [\mathcal{C}_{dd}]_{ijij}, \\ \Delta C_{\text{LR},1}^{ij} &= -\mathcal{N}_{ij}^{-1} \left([\mathcal{C}_{qd}^{(1)}]_{ijij} - \frac{[\mathcal{C}_{qd}^{(8)}]_{ijij}}{2N_c} \right), & \Delta C_{\text{LR},2}^{ij} &= \mathcal{N}_{ij}^{-1} [\mathcal{C}_{qd}^{(8)}]_{ijij},\end{aligned}\tag{21}$$

where \mathcal{N}_{ij} is given in (17). As will be seen in the next section, the $\Delta F = 2$ Wilson coefficients at μ_{ew} receive leading logarithmic contributions via up-type Yukawa-induced mixing from $\psi^2 H^2 D$ operators. The minus signs in the case of VLL and VRR operators reflect the fact that $[\mathcal{C}_{qq}^{(1,3)}]_{ijij}$ and $[\mathcal{C}_{dd}]_{ijij}$ are the coefficients in the Lagrangian and the coefficients C_{VLL}^{ij} and C_{VRR}^{ij} in the Hamiltonian. In the case of LR operators additional Fierz transformations have to be made.

3 Leading RG Effects in SMEFT

The scale dependence of Wilson coefficients is governed by the RG equation

$$\dot{C}_a \equiv (4\pi)^2 \mu \frac{dC_a}{d\mu} = \gamma_{ab} C_b\tag{22}$$

and determined by the ADM γ_{ab} . The ADM is known for SMEFT at one-loop and depends on 1) the quartic Higgs coupling λ [16], 2) the fermion Yukawa couplings to the Higgs doublet [12] and 3) the three gauge couplings $g_{1,2,s}$ [17]. For small $\gamma_{ab}/(4\pi)^2 \ll 1$ the approximate solution retains only the first leading logarithm (1stLLA)

$$C_a(\mu_{\text{ew}}) = \left[\delta_{ab} - \frac{\gamma_{ab}}{(4\pi)^2} \ln \frac{\mu_\Lambda}{\mu_{\text{ew}}} \right] C_b(\mu_\Lambda),\tag{23}$$

which is sufficient as long as the logarithm is not too large, so that also $\gamma_{ab}/(4\pi)^2 \ln \frac{\mu_\Lambda}{\mu_{\text{ew}}} \ll 1$ holds. Numerically one expects the largest enhancements when the ADM γ_{ab} is proportional to the strong coupling $4\pi\alpha_s \sim 1.4$ or the top-Yukawa coupling squared $y_t^2 \sim 1$. The QCD mixing is flavour-diagonal and hence cannot give rise to new genuine phenomenological effects in $\Delta F = 1, 2$ observables. On the other hand, Yukawa couplings are the main source of flavour-off-diagonal interactions responsible for the phenomenology discussed here. The $\text{SU}(2)_L$ gauge interactions induce via ADMs $\gamma_{ab} \propto g_2^2$ and are parametrically suppressed compared to y_t -induced effects, such that we do not consider them here. The suppression is even stronger for $\text{U}(1)_Y$.

Note that the RG equations of SMEFT are in principle a set of coupled differential equations of the RG equations of SM couplings (quartic Higgs, gauge and Yukawa) and the ones of dim-6 Wilson coefficients. The solution of this system in full generality requires the application of numerical methods and the imposition of boundary conditions might be highly nontrivial. The 1stLLA neglects all these “secondary mixing” effects that would be present in the general leading logarithmic approximation (LLA), which would also

resum large logarithms to all orders in couplings. With “secondary mixing” we refer to the situation where an operator \mathcal{O}_A might not have an ADM entry with operator \mathcal{O}_B (no “direct mixing”), but still contributes to the Wilson coefficient $C_B(\mu_{\text{ew}})$, via a direct mixing with some operator \mathcal{O}_C that in turn mixes directly into \mathcal{O}_B .

The most relevant mixing of the $\psi^2 H^2 D$ operators $\mathcal{O}_{Hq}^{(1,3)}$ and \mathcal{O}_{Hd} into $\Delta F = 2$ -mediating ψ^4 operators (13)-(15) proceeds via up-type Yukawa couplings [12], yielding for $(\bar{L}L)(\bar{L}L)$ operators

$$[\dot{\mathcal{C}}_{qq}^{(1)}]_{ijij} = +[Y_u Y_u^\dagger]_{ij} [\mathcal{C}_{Hq}^{(1)}]_{ij} + \dots, \quad (24)$$

$$[\dot{\mathcal{C}}_{qq}^{(3)}]_{ijij} = -[Y_u Y_u^\dagger]_{ij} [\mathcal{C}_{Hq}^{(3)}]_{ij} + \dots, \quad (25)$$

and for $(\bar{L}L)(\bar{R}R)$ operators

$$[\dot{\mathcal{C}}_{qd}^{(1)}]_{ijij} = [Y_u Y_u^\dagger]_{ij} [\mathcal{C}_{Hd}]_{ij} + \dots \quad (26)$$

The dots indicate other terms $\propto \mathcal{C}_{\psi^2 H^2 D}$ that are not proportional to Y_u ⁸ as well as terms $\propto \mathcal{C}_{\psi^4}$, which become relevant in scenarios where these Wilson coefficients are generated at μ_Λ . As can be seen, the two $\Delta F = 2$ operators \mathcal{O}_{dd} and $\mathcal{O}_{qd}^{(8)}$ do not receive direct leading logarithmic contributions. It is well known though that $\mathcal{C}_{qd}^{(8)}$ would be generated via secondary QCD mixing from $\mathcal{C}_{qd}^{(1)}$ [21].

Under the transformation from weak to mass eigenstates for up-type quarks

$$Y_u \stackrel{\text{dim-4}}{\approx} \frac{\sqrt{2}}{v} V_L^u m_U^{\text{diag}} V_R^{u\dagger} = \frac{\sqrt{2}}{v} V_{\text{CKM}}^\dagger m_U^{\text{diag}}, \quad (27)$$

the ADMs transform as

$$[Y_u Y_u^\dagger]_{ij} = \frac{2}{v^2} \sum_{k=u,c,t} m_k^2 V_{ki}^* V_{kj} \approx \frac{2}{v^2} m_t^2 \lambda_t^{ij}, \quad (28)$$

with up-type quark masses m_k . Since the ADMs are needed here for the evolution of dim-6 Wilson coefficients themselves, we have used tree-level relations derived from the dim-4 part of the Lagrangian only, thereby neglecting dim-6 contributions, which would constitute dim-8 corrections in this context. In the sum over k only the top-quark contribution is relevant ($m_{u,c} \ll m_t$), if one assumes that the unitary matrix V is equal to the CKM matrix up to dim-6 corrections.⁹

From (21) and (26) we find that the presence of the RH operator \mathcal{O}_{Hd} at a short distance scale μ_Λ , i.e. $[\mathcal{C}_{Hd}]_{ij}(\mu_\Lambda) \neq 0$, generates through Yukawa RG effects a leading-logarithmic contribution to the LR operator $\mathcal{O}_{\text{LR},1}^{ij}$ at the electroweak scale μ_{ew} , given by

$$\Delta_{\text{1stLLA}} \mathcal{C}_{\text{LR},1}^{ij}(\mu_{\text{ew}}) = v^2 \frac{[\mathcal{C}_{Hd}]_{ij}(\mu_\Lambda)}{\lambda_t^{ij}} x_t \ln \frac{\mu_\Lambda}{\mu_{\text{ew}}}, \quad (29)$$

⁸Note that here Y_u is defined (82) as the hermitean conjugate w.r.t [12].

⁹We expect only tiny contributions from $k = c$ in case that $ij = sd$, for $ij = bd, bs$ such contributions are entirely negligible.

with $v \approx (\sqrt{2}G_F)^{-1/2}$. Similarly, the presence of two operators $\mathcal{O}_{Hq}^{(1)}$ and $\mathcal{O}_{Hq}^{(3)}$ generates via (21), (24) and (25)

$$\Delta_{\text{1stLLA}} C_{\text{VLL}}^{ij}(\mu_{\text{ew}}) = \frac{v^2}{\lambda_t^{ij}} \left([\mathcal{C}_{Hq}^{(1)}]_{ij}(\mu_\Lambda) - [\mathcal{C}_{Hq}^{(3)}]_{ij}(\mu_\Lambda) \right) x_t \ln \frac{\mu_\Lambda}{\mu_{\text{ew}}}. \quad (30)$$

In summary

- \mathcal{O}_{Hd} , corresponding to RH FC quark couplings of the Z , generates the $\Delta F = 2$ left-right operator $O_{\text{LR},1}$, which has numerically enhanced QCD running below μ_{ew} and chirally enhanced hadronic matrix elements;
- $\mathcal{O}_{Hq}^{(1,3)}$, corresponding to LH FC quark couplings of the Z , generate the $\Delta F = 2$ left-left operator O_{VLL} ;
- in the LH case the contribution is $\sim (\mathcal{C}_{Hq}^{(1)} - \mathcal{C}_{Hq}^{(3)}) \propto \Delta_L^u$, contrary to the linear combination $\Delta_L^d \propto (\mathcal{C}_{Hq}^{(1)} + \mathcal{C}_{Hq}^{(3)})$ appearing in the coupling of down-type quarks to the Z in (9).

The latter point implies that the result in (30) and consequently the contributions to $\Delta F = 2$ processes cannot be presented solely in terms of Δ_L^d but must involve due to $\text{SU}(2)_L$ gauge invariance also Δ_L^u . We will return to the phenomenological implications in Section 6.

4 NLO Contributions in SMEFT

In this section we present the results of the calculation of one-loop (NLO) corrections of matrix elements of $\psi^2 H^2 D$ operators to $\Delta F = 2$ transitions in SMEFT, arising in the matching to the $\Delta F = 2$ -EFT. The divergent parts of these matrix elements determine the ADM given in [12], which have been used in Section 3 for the leading RG evolution. Here we calculate the finite parts that also scale with the top-quark Yukawa coupling. While they are not enhanced by a large logarithm, they cancel the μ_{ew} dependence of the leading RG results in (29) and (30). As mentioned in Section 1, these finite parts involve novel gauge-independent functions. Similar NLO matching corrections in the context of matching SMEFT onto low-energy EFTs have been also calculated for operators entering $\mu \rightarrow e\gamma$ [22], $\mu \rightarrow e\nu_\mu\bar{\nu}_e$ [23], which is used to determine G_F , anomalous triple gauge couplings in rare decays $d_j \rightarrow d_i + (\gamma, \ell^+\ell^-, \nu\bar{\nu})$ [24] and extensively for many $\Delta B = 1, 2$ processes in [19]. Regarding $\Delta F = 2$ transitions, the latter work has considered only NLO matrix elements of ψ^4 operators ($\mathcal{O}_{qu}^{(1,8)}$ and $\mathcal{O}_{ud}^{(1,8)}$) to the matching of SMEFT and $\Delta F = 2$ -EFT. Very recently, the NLO matching corrections of \mathcal{O}_{Hud} have been calculated for $\Delta F = 1, 2$ processes in [25].

4.1 $\Delta F = 2$ NLO matching

The classes of diagrams we consider are shown in Fig. 1. Details on the Feynman rules of the operators \mathcal{O}_{Hd} and $\mathcal{O}_{Hq}^{(1,3)}$ are provided in Appendix A in the mass eigenbasis for gauge

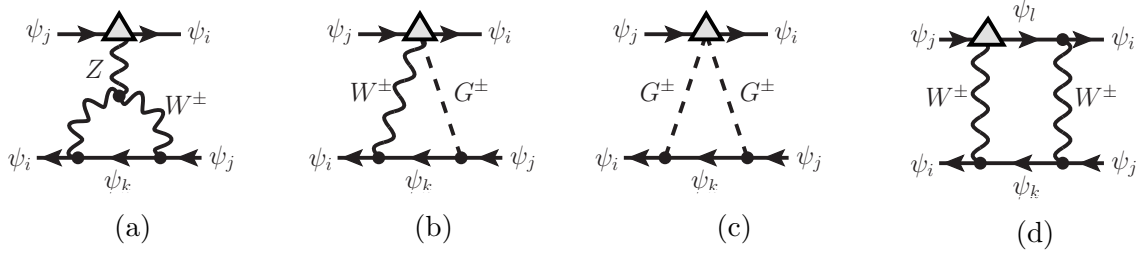


Figure 1: Classes of diagrams (up to permutations and insertions flipped to lower fermion-line) contributing to $\Delta F = 2$ one-loop matrix elements of the operators \mathcal{O}_{Hd} and $\mathcal{O}_{Hq}^{(1,3)}$. Operator insertions are depicted by triangles and SM couplings by small dots. Diagrams (1a) and (1d) appear also with replacement of each $W^\pm \rightarrow G^\pm$ and further (1a) with the Z -boson emitted from the virtual ψ_k . The operators \mathcal{O}_{Hd} and $\mathcal{O}_{Hq}^{(1)}$ generate diagrams (1a – 1c), whereas operator $\mathcal{O}_{Hq}^{(3)}$ generates diagrams (1a, 1c, 1d).

bosons and quarks after EWSB. Among the 1-particle-irreducible (1PI) diagrams only the diagram (1c) gives rise to divergences, which are absorbed into counterterms and are known from the ADM calculation [12]. The heavy-particle-reducible (HPR) diagram (1a) is well-known from the SM calculation and gives rise to the gauge-dependent Inami-Lim function $C(x_t)$. As usual, it requires the inclusion of the counterterm of the flavour-off-diagonal wave-function renormalization constant $\psi_j \rightarrow \psi_i$. The external momenta and the up- and charm-quark masses are set to zero throughout. We do not use the background-field method, such that top-, charm- and up-quark contributions are not separately finite [26], but their sum is finite after GIM-summation, i.e. exploiting the unitarity of the CKM matrix V . The box diagrams (1d) are finite, but not gauge-independent. We perform our calculation in general R_ξ gauge for electroweak gauge bosons in order to verify explicitly the gauge independence of the final results after GIM-summation.

The result of the one-loop matching modifies the tree-level matching relations (21) as

$$\Delta C_c(\mu_{\text{ew}}) = \sum_{a \in \psi^4} G_a^{(0,c)} \mathcal{C}_a^{\psi^4}(\mu_{\text{ew}}) + \sum_{b \in \psi^2 H^2 D} G_b^{(1,c)}(x_t, \mu_{\text{ew}}), \quad (31)$$

with $c = \text{VLL, LR, 1}$ and generation-indices omitted for brevity. In this equation

- $G_a^{(0,c)}$ is the tree-level matrix element of the ψ^4 operator \mathcal{O}_a to the $\Delta F = 2$ -EFT operator O_c , which can be read off from (21);
- $G_b^{(1,c)}(x_t, \mu_{\text{ew}})$ is the one-loop matrix element of the $\psi^2 H^2 D$ operator \mathcal{O}_b to O_c ;
- the μ_{ew} dependence of $G_b^{(1,c)}(x_t, \mu_{\text{ew}})$ cancels the one present in $\mathcal{C}_a^{\psi^4}(\mu_{\text{ew}})$ due to (29) and (30).

We find for \mathcal{O}_{Hd}

$$G_{Hd,ij}^{(1,\text{LR1})}(x_t, \mu_{\text{ew}}) = v^2 \frac{[\mathcal{C}_{Hd}]_{ij}(\mu_{\text{ew}})}{\lambda_t^{ij}} x_t H_1(x_t, \mu_{\text{ew}}), \quad (32)$$

and similarly for $\mathcal{O}_{Hq}^{(1)}$

$$G_{Hq^{(1)},ij}^{(1,\text{VLL})}(x, \mu_{\text{ew}}) = v^2 \frac{[\mathcal{C}_{Hq}^{(1)}]_{ij}(\mu_{\text{ew}})}{\lambda_t^{ij}} x_t H_1(x_t, \mu_{\text{ew}}). \quad (33)$$

In the case of $\mathcal{O}_{Hq}^{(3)}$

$$\begin{aligned} G_{Hq^{(3)},ij}^{(1,\text{VLL})}(x, \mu_{\text{ew}}) = & -\frac{v^2}{\lambda_t^{ij}} x_t \left[[\mathcal{C}_{Hq}^{(3)}]_{ij}(\mu_{\text{ew}}) H_2(x_t, \mu_{\text{ew}}) \right. \\ & \left. - \frac{2S_0(x_t)}{x_t} \sum_m \left(\lambda_t^{im} [\mathcal{C}_{Hq}^{(3)}]_{mj}(\mu_{\text{ew}}) + [\mathcal{C}_{Hq}^{(3)}]_{im}(\mu_{\text{ew}}) \lambda_t^{mj} \right) \right], \end{aligned} \quad (34)$$

where the second term is due to the box diagrams in Fig. 1d, proportional to the gauge-independent SM Inami-Lim function $S_0(x_t)$ (20) and moreover involving not only the coefficients $[\mathcal{C}_{Hq}^{(3)}]_{ij}$, but also those with $m \neq i$ and $m \neq j$.

The expressions of the $\Delta F = 2$ Wilson coefficients at NLO are then obtained by inserting the 1stLLA results (29) and (30) together with the NLO matrix elements $G_b^{(1,c)}(x_t, \mu_{\text{ew}})$ into (31). Furthermore, in $G_b^{(1,c)}(x_t, \mu_{\text{ew}})$ we neglect “self-mixing” and approximate $\mathcal{C}_{\psi^2 H^2 D}(\mu_{\text{ew}}) \approx \mathcal{C}_{\psi^2 H^2 D}(\mu_\Lambda)$ – see (23) and (91) – which is numerically small, such that finally

$$\Delta C_{\text{LR},1}^{ij}(\mu_{\text{ew}}) = v^2 \frac{[\mathcal{C}_{Hd}]_{ij}}{\lambda_t^{ij}} x_t \left\{ \ln \frac{\mu_\Lambda}{\mu_{\text{ew}}} + H_1(x_t, \mu_{\text{ew}}) \right\}, \quad (35)$$

$$\begin{aligned} \Delta C_{\text{VLL}}^{ij}(\mu_{\text{ew}}) = & \frac{v^2}{\lambda_t^{ij}} x_t \left\{ [\mathcal{C}_{Hq}^{(1)} - \mathcal{C}_{Hq}^{(3)}]_{ij} \ln \frac{\mu_\Lambda}{\mu_{\text{ew}}} + [\mathcal{C}_{Hq}^{(1)}]_{ij} H_1(x_t, \mu_{\text{ew}}) - [\mathcal{C}_{Hq}^{(3)}]_{ij} H_2(x_t, \mu_{\text{ew}}) \right. \\ & \left. + \frac{2S_0(x_t)}{x_t} \sum_m \left(\lambda_t^{im} [\mathcal{C}_{Hq}^{(3)}]_{mj} + [\mathcal{C}_{Hq}^{(3)}]_{im} \lambda_t^{mj} \right) \right\}, \end{aligned} \quad (36)$$

where we have omitted the argument μ_Λ for all $\mathcal{C}_{\psi^2 H^2 D}$ for brevity.

There are two gauge-independent functions¹⁰ that depend on μ_{ew} :

$$H_1(x, \mu_{\text{ew}}) = \ln \frac{\mu_{\text{ew}}}{M_W} - \frac{x-7}{4(x-1)} - \frac{x^2-2x+4}{2(x-1)^2} \ln x, \quad (37)$$

$$H_2(x, \mu_{\text{ew}}) = \ln \frac{\mu_{\text{ew}}}{M_W} + \frac{7x-25}{4(x-1)} - \frac{x^2-14x+4}{2(x-1)^2} \ln x. \quad (38)$$

The cancellation of the μ_{ew} -dependence between the 1stLLA contribution $\propto \ln(\mu_\Lambda/\mu_{\text{ew}})$ and the NLO functions $H_{1,2}(x_t, \mu_{\text{ew}})$ can be easily seen in (35) and (36). However, we keep μ_{ew} on the l.h.s in (35) and (36) to indicate the scale for the RG QCD evolution in the $\Delta F = 2$ -EFTs down to low energies. In this case the cancellation of μ_{ew} dependence involves QCD effects and has been known [18].

¹⁰The function H_1 is also present in different context in [19], Eq.(4.3).

For convenience we give the composition of $H_{1,2}$ in terms of the gauge-dependent Inami-Lim function $C(x, \xi_W)$ [2] and some remainder functions $\tilde{H}_{1,2}$ due to diagrams Figs. 1b – 1d:

$$H_i(x, \mu_{\text{ew}}) = \frac{a_i}{x} C(x, \xi_W) + \tilde{H}_i(x, \mu_{\text{ew}}, \xi_W), \quad (39)$$

with $a_1 = -8$ and $a_2 = 8$. The $\tilde{H}_{1,2}$ can be easily calculated from $H_{1,2}$ and the knowledge of $C(x, \xi_W)$ for every choice of ξ_W , in particular

$$C(x, 1) = \frac{x}{8} \left(\frac{x-6}{x-1} + \frac{3x+2}{(x-1)^2} \ln x \right), \quad (40)$$

with $C(x_t, 1) \approx 0.78$ for $x_t \approx 4$.

4.2 Numerical Impact of NLO Contributions

Fig. 2 illustrates the cancellation of the scale dependence present at LO: shown are the coefficients (c_i) of \mathcal{C}_{Hd} in $C_{\text{LR},1}(\mu_{\text{ew}})$, as well $\mathcal{C}_{Hq}^{(1)}$ and $-\mathcal{C}_{Hq}^{(3)}$ in ΔC_{VLL} for LO and NLO. The absolute size of the NLO contribution $H_1(x_t, \mu_{\text{ew}})$ is close to zero for $\mu_{\text{ew}} = m_t$, but cancels the logarithm which induces otherwise an uncertainty of about $\sim 10\%$ related to the choice of this scale. The NLO correction involving $H_2(x_t, \mu_{\text{ew}})$ is sizable everywhere. At the order we are working, the renormalization scheme of the top quark mass is not specified as far as the SMEFT contributions are concerned and hence in principle every scheme can be used. Here we use the value in the $\overline{\text{MS}}$ scheme that enters also the SM contribution. The leading μ dependence of this top-quark mass is governed by QCD corrections that will be cancelled by the inclusion of NLO-QCD corrections to the SMEFT-contribution at the 2-loop level, being of higher order in this context. Therefore we keep the scale of the top-quark mass fixed in Fig. 2. However, we include NLO QCD corrections to the SM contribution in the numerical evaluations.

The relative size of the NLO corrections w.r.t. the 1stLLA depends not only on the scale μ_{ew} at which the contributions are evaluated, but also on the high scale μ_Λ . For example from (35) follows with $x_t \approx 4$

$$\Delta C_{\text{LR},1}^{ij}(\mu_{\text{ew}}) = v^2 \frac{[\mathcal{C}_{Hd}]_{ij}(\mu_\Lambda)}{\lambda_t^{ij}} x_t \left[\left\{ \begin{array}{l} 2.5 \text{ for } \mu_\Lambda = 1 \text{ TeV} \\ 4.8 \text{ for } \mu_\Lambda = 10 \text{ TeV} \end{array} \right\} - 0.7 \right], \quad (41)$$

where the values in braces correspond to the $\ln(\mu_\Lambda/M_W)$ for the two choices of μ_Λ and the NLO contribution due to $H_1(x_t, M_W) = -0.7$ constitutes a destructive relative correction of 28% to 15% for μ_Λ in the range of 1 TeV to 10 TeV. The same holds for $\Delta C_{\text{VLL}}^{ij}(\mu_{\text{ew}})$ when generated by $\mathcal{C}_{Hq}^{(1)}$.

On the other hand, for $\mathcal{C}_{Hq}^{(3)}$ one part of the NLO matching contributions is

$$\ln \frac{\mu_\Lambda}{M_W} + H_2(x_t, M_W) = \left\{ \begin{array}{l} 2.5 \text{ for } \mu_\Lambda = 1 \text{ TeV} \\ 4.8 \text{ for } \mu_\Lambda = 10 \text{ TeV} \end{array} \right\} + 3.0, \quad (42)$$

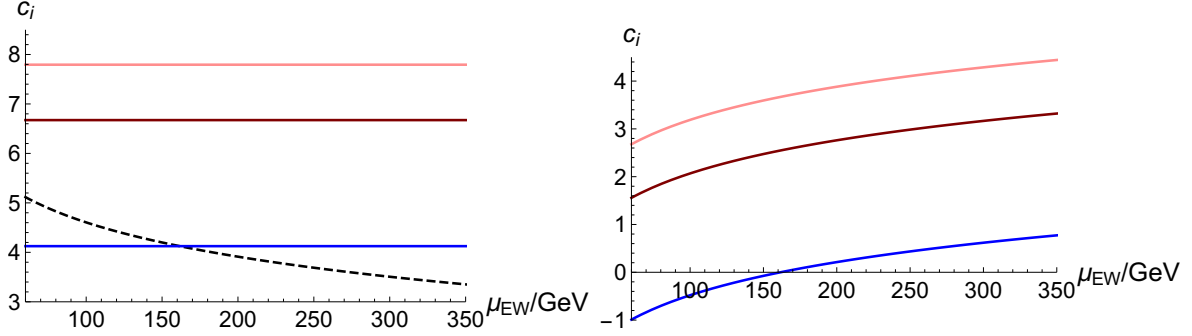


Figure 2: The μ_{ew} -dependence of the coefficients (c_i) of \mathcal{C}_{Hd} in $\Delta C_{\text{LR},1}(\mu_{\text{ew}})$, as well $\mathcal{C}_{Hq}^{(1)}$ and $-\mathcal{C}_{Hq}^{(3)}$ in $\Delta C_{\text{VLL}}(\mu_{\text{ew}})$ for LO and NLO, with $\mu_\Lambda = 10$ TeV. The black dashed curve in the left figure is the LO contribution, which is equal for all three coefficients. In the left (right) figure, the blue line is the LO+NLO (NLO) contribution of \mathcal{C}_{Hd} in $\Delta C_{\text{LR},1}$ as well as $\mathcal{C}_{Hq}^{(1)}$ in ΔC_{VLL} , both flavour universal. The dark red line corresponds to LO+NLO (NLO) contribution of $[\mathcal{C}_{Hq}^{(3)}]_{ij}$ in ΔC_{VLL} for $i = b, j = d, s$, while the light red line is for $ij = sd$. Note that the top-quark mass is kept fixed in this plot.

that is, of order 100% and constructive to the 1stLLA term. The second part due to the box contribution proportional to

$$\frac{2S_0(x_t)}{x_t} \rightarrow 1.1 \quad (43)$$

depends on i and j and an additional CKM suppression might occur. It is instructive to list the Cabibbo suppression, $\lambda_C \approx 0.2$, of each term in the sum of (36) for the three cases $ij = bs, bd, sd$

$$\begin{aligned} ij = bs : & \quad \mathcal{O}(\lambda_C^2) \cdot [\mathcal{C}_{Hq}^{(3)}]_{bb,ss}, \quad \mathcal{O}(1) \cdot [\mathcal{C}_{Hq}^{(3)}]_{bs}, \quad \mathcal{O}(\lambda_C^3) \cdot [\mathcal{C}_{Hq}^{(3)}]_{sd}, \quad \mathcal{O}(\lambda_C^5) \cdot [\mathcal{C}_{Hq}^{(3)}]_{bd}; \\ ij = bd : & \quad \mathcal{O}(\lambda_C^3) \cdot [\mathcal{C}_{Hq}^{(3)}]_{bb,dd}, \quad \mathcal{O}(1) \cdot [\mathcal{C}_{Hq}^{(3)}]_{bd}, \quad \mathcal{O}(\lambda_C^2) \cdot [\mathcal{C}_{Hq}^{(3)}]_{sd}, \quad \mathcal{O}(\lambda_C^5) \cdot [\mathcal{C}_{Hq}^{(3)}]_{bs}; \\ ij = sd : & \quad \mathcal{O}(\lambda_C^5) \cdot [\mathcal{C}_{Hq}^{(3)}]_{ss,dd}, \quad \mathcal{O}(\lambda_C^2) \cdot [\mathcal{C}_{Hq}^{(3)}]_{bd}, \quad \mathcal{O}(\lambda_C^3) \cdot [\mathcal{C}_{Hq}^{(3)}]_{bs}, \quad \mathcal{O}(\lambda_C^4) \cdot [\mathcal{C}_{Hq}^{(3)}]_{sd}. \end{aligned} \quad (44)$$

It can be seen that for B -meson mixing, $ij = bd, bs$, there will be one term $\lambda_t^{bb} [\mathcal{C}_{Hq}^{(3)}]_{bj} \sim \mathcal{O}(1) \times [\mathcal{C}_{Hq}^{(3)}]_{bj}$ without Cabibbo suppression for the $[\mathcal{C}_{Hq}^{(3)}]_{bj}$ itself that mediates the process in 1stLLA, whereas all other contributions are suppressed by at least $\mathcal{O}(\lambda_C^2)$. For Kaon-mixing, $ij = sd$, the largest CKM combination will be $\lambda_t^{sb} [\mathcal{C}_{Hq}^{(3)}]_{bd} \sim \lambda_C^2 [\mathcal{C}_{Hq}^{(3)}]_{bd}$ with quadratic Cabibbo suppression. Although at NLO for a given transition ij the $[\mathcal{C}_{Hq}^{(3)}]_{mn}$ with $mn \neq ij$ are at least suppressed by $\mathcal{O}(\lambda_C^2)$ in (36), it cannot be excluded that the Cabibbo suppression can be lifted in the case that some of the $[\mathcal{C}_{Hq}^{(3)}]_{mn}$ are very hierarchical too, as already mentioned below (10), and thus might become even numerically leading contributions. In the remainder of this work we will always assume that this is not the case, and hence neglect all Cabibbo-suppressed contributions, but for the most general situation a global analysis would be required that puts simultaneous constraints on all $\mathcal{C}_{Hq}^{(3)}$. The neglected contributions could be relevant for example if flavour-diagonal processes

put significantly less severe bounds on $[\mathcal{C}_{Hq}^{(3)}]_{kk}$ ($kk = bb, ss, dd$) than flavour-changing processes on the flavour-off-diagonal couplings $[\mathcal{C}_{Hq}^{(3)}]_{ij}$ ($i \neq j$). The numerical effect on $\Delta F = 2$ observables is hard to predict without the full analysis; however, for example flavour-diagonal contributions $[\mathcal{C}_{Hq}^{(3)}]_{ss, dd}$ in Kaon mixing are suppressed by $\mathcal{O}(\lambda_C^5)$ and hence much less likely to invalidate our assumption, compared to B_s and B_d mixing where the corresponding contributions are only suppressed by $\mathcal{O}(\lambda_C^2)$ and $\mathcal{O}(\lambda_C^3)$, respectively. Note that these considerations do not affect most of our conclusions; specifically, none of the plots presented for the right-handed scenario in Section 6.3.1 is changed. Concerning the left-handed scenario in Section 6.3.2, the constraints in Fig. 9 derived from $\Delta F = 2$ could be changed, but not the ones from $\Delta F = 1$ processes and similarly for Fig. 10.

4.3 NLO Contributions in VLQ Models

In this section we would like to illustrate the model dependence of NLO contributions in LH and RH scenarios in the context of vector-like quark (VLQ) models. To this end we use the results for the coefficients $\mathcal{C}_{Hq}^{(1,3)}$ and \mathcal{C}_{Hd} evaluated in VLQ models [14, 15] of one singlet, one doublet and two triplets:

$$D(1, -1/3), \quad Q_d(2, -5/6), \quad T_d(3, -1/3), \quad T_u(3, +2/3), \quad (45)$$

where the transformation properties are indicated as $(\text{SU}(2)_L, \text{U}(1)_Y)$ and all VLQs are triplets under $\text{SU}(3)_c$. They interact with SM quarks (q_L, u_R, d_R) and the Higgs doublet via Yukawa interactions

$$-\mathcal{L}_{\text{Yuk}}(H) = \left(\lambda_i^D H^\dagger \bar{D}_R + \lambda_i^{T_d} H^\dagger \bar{T}_{dR} + \lambda_i^{T_u} \tilde{H}^\dagger \bar{T}_{uR} \right) q_L^i + \bar{d}_R^i \lambda_i^{Q_d} \tilde{H}^\dagger Q_{dL} + \text{h.c.} \quad (46)$$

The complex-valued Yukawa couplings λ_i^{VLQ} give rise to mixing with the SM quarks and consequently to FC quark couplings of Z . The Wilson coefficients $\mathcal{C}_{Hq}^{(1,3)}$ and \mathcal{C}_{Hd} are given in terms of Yukawa couplings λ_i^{VLQ} and the VLQ mass M_{VLQ} . The Wilson coefficients are [14, 15]

$$\begin{aligned} D : \quad [\mathcal{C}_{Hq}^{(1)}]_{ij} &= [\mathcal{C}_{Hq}^{(3)}]_{ij} = -\frac{1}{4} \frac{\lambda_i^* \lambda_j}{M^2}, & Q_d : \quad [\mathcal{C}_{Hd}]_{ij} &= -\frac{1}{2} \frac{\lambda_i \lambda_j^*}{M^2}, \\ T_d : \quad [\mathcal{C}_{Hq}^{(1)}]_{ij} &= -3 [\mathcal{C}_{Hq}^{(3)}]_{ij} = -\frac{3}{8} \frac{\lambda_i^* \lambda_j}{M^2}, & T_u : \quad [\mathcal{C}_{Hq}^{(1)}]_{ij} &= 3 [\mathcal{C}_{Hq}^{(3)}]_{ij} = +\frac{3}{8} \frac{\lambda_i^* \lambda_j}{M^2}, \end{aligned} \quad (47)$$

at the high scale $\mu_\Lambda \approx M_{\text{VLQ}}$.

In the following we use these Wilson coefficients in (36) in order to demonstrate the size of NLO corrections in specific models. In the $\text{VLQ} = D$ one finds that the 1stLLA is vanishing such that the whole effect is first generated at NLO and lacks the enhancement by the large logarithm:

$$\begin{aligned} \Delta C_{\text{VLL}}^{ij} &= -\frac{x_t}{4} \frac{\lambda_i^* \lambda_j}{\lambda_t^{ij}} \frac{v^2}{M^2} \left[H_1(x_t, M_W) - H_2(x_t, M_W) + \frac{2S_0(x_t)}{x_t} + \dots \right] \\ &= -\frac{x_t}{4} \frac{\lambda_i^* \lambda_j}{\lambda_t^{ij}} \frac{v^2}{M^2} [-0.7 - 3.0 + 1.1 + \dots] \approx -\frac{x_t}{4} \frac{\lambda_i^* \lambda_j}{\lambda_t^{ij}} \frac{v^2}{M^2} \times (-2.6 + \dots), \end{aligned} \quad (48)$$

where we have assumed that one of the indices $i, j = b$, see comments below (43). For example in scenario VLQ = T_d one finds (using $\mu_{\text{ew}} = M_W$)

$$\begin{aligned} \Delta C_{\text{VLL}}^{ij} &= -\frac{3x_t}{8} \frac{\lambda_i^* \lambda_j}{\lambda_t^{ij}} \frac{v^2}{M^2} \left[\frac{4}{3} \ln \frac{\mu_\Lambda}{M_W} + H_1(x_t, M_W) + \frac{H_2(x_t, M_W)}{3} - \frac{2S_0(x_t)}{3x_t} + \dots \right] \\ &\approx -\frac{3x_t}{8} \frac{\lambda_i^* \lambda_j}{\lambda_t^{ij}} \frac{v^2}{M^2} \left[\left\{ \begin{array}{l} 3.3 \text{ for } \mu_\Lambda = 1 \text{ TeV} \\ 6.4 \text{ for } \mu_\Lambda = 10 \text{ TeV} \end{array} \right\} - 0.1 + \dots \right] \end{aligned} \quad (49)$$

and analogously for VLQ = T_u

$$\begin{aligned} \Delta C_{\text{VLL}}^{ij} &= \frac{3x_t}{8} \frac{\lambda_i^* \lambda_j}{\lambda_t^{ij}} \frac{v^2}{M^2} \left[\frac{2}{3} \ln \frac{\mu_\Lambda}{M_W} + H_1(x_t, M_W) - \frac{H_2(x_t, M_W)}{3} + \frac{2S_0(x_t)}{3x_t} + \dots \right] \\ &\approx \frac{3x_t}{8} \frac{\lambda_i^* \lambda_j}{\lambda_t^{ij}} \frac{v^2}{M^2} \left[\left\{ \begin{array}{l} 1.7 \text{ for } \mu_\Lambda = 1 \text{ TeV} \\ 3.2 \text{ for } \mu_\Lambda = 10 \text{ TeV} \end{array} \right\} - 1.3 + \dots \right]. \end{aligned} \quad (50)$$

These results show that depending on the relative size of $\mathcal{C}_{Hq}^{(1)}$ w.r.t. $\mathcal{C}_{Hq}^{(3)}$, NLO corrections can cancel or be comparable to the 1stLLA contributions. Moreover, the comparison of D with $T_{u,d}$ shows that the NLO corrections by themselves indeed can be relevant even if the 1stLLA contribution cancels in models with $\mathcal{C}_{Hq}^{(1)} - \mathcal{C}_{Hq}^{(3)} = 0$.¹¹

For the RH scenario Q_d there is only one coefficient \mathcal{C}_{Hd} such that the effect has been already discussed in (41).

5 Comparison with the Literature

This section is devoted to the comparison of the SMEFT approach to FC quark couplings of the Z with previous studies of this NP scenario in the context of rare Kaon and B -meson $\Delta F = 1, 2$ processes [8–11]. We will focus in particular on the parameterization of these effects given in (11), to which we will refer in the following as “simplified models”.

The SMEFT is well defined by the requirement that the low-energy field content corresponds to the one of the SM, the imposition of the SM gauge group G_{SM} and the presence of a mass gap between the electroweak scale and the new dynamics $\mu_{\text{ew}} \ll \mu_\Lambda$. Further, the RG equations yield the relations between Wilson coefficients at both scales. In comparison, the simplified models lack quantum-field-theoretical principles and constitute simply a postulation of new FC quark couplings of the Z . They leave questions open regarding for instance the appropriate scale for the couplings and the implementation of gauge invariance under the SM gauge group. As a consequence their application beyond tree-level seems problematic and one should assume the couplings Δ_χ^ψ ($\psi = u, d$ and $\chi = L, R$) in (11) to be at μ_{ew} .

Consider the example of $\Delta F = 1$ decays $\psi_j \rightarrow \psi_i f \bar{f}$ (with $\psi = u, d$ and $f = \nu, \ell, q$), mediated by the tree-level Z -exchange depicted in Fig. 3a. The FC coupling is due to either dim-6 SMEFT operators or Δ_χ^ψ couplings in simplified models, whereas the

¹¹Note that in full generality such a relation holds only at a specific scale, here μ_Λ , but self-mixing is a loop-suppressed correction in this context.

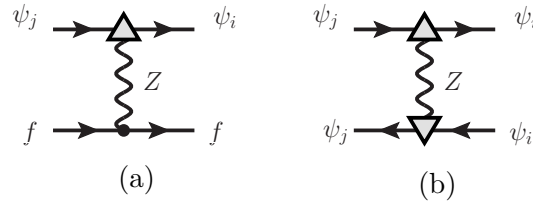


Figure 3: Tree-level mediated $\Delta F = 1$ diagram (3a) and $\Delta F = 2$ diagram (3b) processes as used in simplified models. Insertions of FC quark couplings of Z of simplified models are depicted by the triangle and SM couplings by small dots.

other coupling is the SM gauge coupling $Z f \bar{f} \propto g_Z$ that derives from gauge invariance of the dim-4 SM Lagrangian under G_{SM} . In the SMEFT case, we have neglected double insertions of dim-6 operators. We have also approximated the flavour-diagonal Z coupling in the simplified model by its SM value. At this level, the results obtained in previous studies of $\Delta F = 1$ transitions based on simplified models can be translated into constraints on the SMEFT Wilson coefficients using (12).

$\Delta F = 2$ processes provide important complementary constraints w.r.t $\Delta F = 1$, and depending on the presence of new LH and/or RH interactions the correlations might change. In simplified models they are mediated via a double-insertion, see Fig. 3b, and the amplitude scales as $(\Delta_\chi^\psi)^2$. In SMEFT one has in general local $(\Delta F = 2)$ - ψ^4 operators (31) with potential NLO corrections from other classes of operators. In the special case of FC quark couplings of the Z these ψ^4 operators are generated via Yukawa-enhanced RG evolution from $\psi^2 H^2 D$ operators – see (29) and (30) – and the $\Delta F = 2$ amplitude scales as $\mathcal{C}_{\psi^2 H^2 D}$ and hence linearly in Δ_χ^ψ , see (12). This linear dependence remains at NLO in SMEFT.

The quadratic dependence of $\Delta F = 2$ amplitudes on Δ_χ^ψ present in the results of simplified models in the literature is absent in SMEFT at the level of single dim-6 operator insertions and arises in SMEFT when going to the dim-8 level by inserting two dim-6 operators. The dim-8 contributions to $\Delta F = 2$ processes will become more important in SMEFT for smaller scales $\mu_{\text{ew}} \lesssim \mu_\Lambda$. In fact, since the dim-6 Yukawa-generated contributions are one-loop suppressed one might ask at which scale the dim-8 contributions start to have similar impact. Equating the naive dimensional scalings of dim-6 one-loop suppressed contributions, $v^2/\mu_\Lambda^2 (4\pi)^{-2}$, with the ones of dim-8 contributions, v^4/μ_Λ^4 , yields a transition regime $\mu_\Lambda \sim 4\pi v \approx 3 \text{ TeV}$.

Lets consider first the SMEFT with $\mu_\Lambda \gtrsim 4\pi v$ and continue our comparison with the simplified model. In this case, both approaches generate in general different operators in the $\Delta F = 2$ -EFT (16) below μ_{ew} , as listed in Table 1. A major difference occurs here for RH interactions, where simplified models generate O_{VRR} and SMEFT $O_{\text{LR},1}$. The latter has a large enhancement under RG evolution in QCD below μ_{ew} and chirally enhanced matrix elements compared to O_{VRR} , such that phenomenology completely changes, especially in the Kaon sector – see Section 6.1. But also for LH interactions closer inspection shows that the involved couplings are the ones of up-type quarks, Δ_L^u , if one uses (12) to relate SMEFT Wilson coefficients to Δ_χ^ψ couplings in the 1stLLA result (30). Indeed, while in the simplified approach the LH- Z couplings involved are just $\propto (\mathcal{C}_{Hq}^{(1)} + \mathcal{C}_{Hq}^{(3)})$,

	Simplified models	SMEFT (dim-6)
$\Delta F = 2$ -amplitude	$\sim (\Delta_\chi^\psi)^2$	$\sim \Delta_\chi^\psi$
LH	$O_{\text{VLL}} \sim (\Delta_L^d)^2$	$O_{\text{VLL}} \sim \Delta_L^u$
RH	$O_{\text{VRR}} \sim (\Delta_R^d)^2$	$O_{\text{LR},1} \sim \Delta_R^d$
LH+RH	$O_{\text{VLL}} \sim (\Delta_L^d)^2, O_{\text{VRR}} \sim (\Delta_R^d)^2,$ $O_{\text{LR},1} \sim (\Delta_L^d \Delta_R^d)$	$O_{\text{VLL}} \sim \Delta_L^u$ $O_{\text{LR},1} \sim \Delta_R^d$

Table 1: Comparison of simplified models and SMEFT (assuming $\mu_\Lambda \gtrsim 4\pi v$) for down-type quark $\Delta F = 2$ processes. Scaling of the $\Delta F = 2$ amplitude in terms of couplings Δ_χ^ψ ($\psi = u, d$ and $\chi = L, R$) from (11). Operators generated in $\Delta F = 2$ -EFT below μ_{ew} by LH, RH or LH+RH scenarios and their scaling with Δ_χ^ψ (in 1stLLA for SMEFT, i.e. neglecting NLO corrections).

the leading RG contribution in question is $\propto (\mathcal{C}_{Hq}^{(1)} - \mathcal{C}_{Hq}^{(3)})$ and therefore proportional to up-quark couplings rather than down-quark couplings as seen in (12).

If one considers the SMEFT with $\mu_\Lambda \lesssim 4\pi v$, double insertions of dim-6 operators are expected to be of similar size or even dominate over loop contributions with one dim-6 insertion. The quadratic dependence on Δ_χ^ψ via the dim-8 contributions is then present in the amplitude, resembling the simplified model approach.

After having established the conditions for a correspondence of simplified models and SMEFT, we will next compare our results with the ones in [11] on the issue of gauge dependence and renormalization scale dependence stressed in points 1. and 2. of Section 1. These authors calculated first the contributions in Fig. 1a in simplified models for RH and LH scenarios. Adding pure NP contributions from tree-level exchange considered in [8] one finds then

$$\mathcal{N}_{ij} C_{\text{VRR}}^{ij} = \frac{[\Delta_R^d]_{ij} [\Delta_R^d]_{ij}}{2M_Z^2}, \quad \mathcal{N}_{ij} C_{\text{LR},1}^{ij} = \frac{[\Delta_L^d(\text{SM})]_{ij} [\Delta_R^d]_{ij}}{M_Z^2}, \quad (51)$$

$$\mathcal{N}_{ij} C_{\text{VLL}}^{ij} = \frac{[\Delta_L^d]_{ij} [\Delta_L^d]_{ij}}{2M_Z^2} + \frac{[\Delta_L^d(\text{SM})]_{ij} [\Delta_L^d]_{ij}}{M_Z^2}, \quad (52)$$

for RH and LH scenarios, respectively. Here the FC $d_j \rightarrow d_i Z$ vertex of the SM arises from the lower part of Fig. 1a,

$$[\Delta_L^d(\text{SM})]_{ij} = \lambda_t^{ij} \frac{g_2^3}{8\pi^2 \cos \theta_W} C(x_t, \xi_W), \quad (53)$$

where θ_W denotes the weak mixing angle and $C(x_t, \xi_W = 1)$, given in (40), is gauge-dependent.¹² In the second version of their paper they included the diagrams (1b) and (1c) obtaining a gauge independent result for the NLO contributions to the coefficients

¹²Note that $[\Delta_L^d(\text{SM})]_{ij} \sim +g_2^3 C(x_t)$ in (53) corresponds to the definition of the covariant derivative in (81).

\mathcal{C}_{Hd} and $\mathcal{C}_{Hq}^{(1)}$, which agrees with ours, but $\mathcal{C}_{Hq}^{(3)}$ has not been considered there. Even prior to the second version of this paper we have suggested how their original results could be corrected. Indeed using the relations in (12) we can cast our results into the ones of [11]. We find in the RH scenario the following replacement in (51):

$$[\Delta_L^d(\text{SM})]_{ij} \rightarrow \frac{\lambda_t^{ij} g_2^3}{8\pi^2 \cos \theta_W} \left[C(x_t, \xi_W) - \frac{x_t}{8} \left(\ln \frac{\mu_\Lambda}{\mu_{\text{ew}}} + \tilde{H}_1(x_t, \mu_{\text{ew}}, \xi_W) \right) \right], \quad (54)$$

with the latter coupling including LO and NLO corrections obtained in SMEFT. As discussed before, this combination of C with \tilde{H}_1 is gauge-independent and μ_{ew} -independent. The numerical values for $\xi_W = 1$ and $x_t \approx 4$ are

$$C(x_t, \xi_W) - \frac{x_t}{8} \tilde{H}_1(x_t, M_W, \xi_W) \approx 0.78 - 0.41, \quad (55)$$

suggesting that a gauge-independent result would have been at least about a factor of two smaller than the one used in the original version of [11]. Further, the logarithm in (54) will typically dominate for reasonable values of μ_Λ , flipping the sign of $[\Delta_L^d(\text{SM})]_{ij}$ compared to [11]. Although our comparison suggests that one can correct the gauge dependence in the simplified model by the replacement (54), conceptually this does not seem meaningful.

Thus the issue of gauge dependence of the NLO correction has been resolved. Unfortunately, the present result in [11], although gauge independent, exhibits a very large renormalization scale dependence, simply because the authors decided not to include the *dominant* LO (1stLLA) top-Yukawa RG effects above the electroweak scale, given in (54) by the term $\propto \ln \mu_\Lambda / \mu_{\text{ew}}$. Furthermore, the renormalization scale μ in their paper, equivalent to the matching scale μ_{ew} in our paper, has been set to 1 TeV. In this case the NLO correction by itself will be of similar size and have the same sign as the (LO + NLO) result in (54). However, the choice $\mu_{\text{ew}} = 1$ TeV is clearly not allowed, because at this matching scale one cannot integrate out Z , W and the top-quark, which have masses one order of magnitude smaller. Moreover, neglecting the $\propto \ln \mu_\Lambda / \mu_{\text{ew}}$ is not allowed from the point of view of SMEFT, because it would imply that dimension six operators are generated at $\mu_\Lambda = \mu_{\text{ew}}$.

Indeed, returning to the right plot in Fig. 2 (blue line for \mathcal{C}_{Hd}), one can see that even varying μ_{ew} in an admissible range, the neglect of RG Yukawa effects above the electroweak scale yields a very strong μ_{ew} dependence. In particular, for scales close to m_t , the NLO corrections considered in [11] vanish. The fact that with a particular choice of matching scale NLO corrections can often be absorbed into the leading term is well known in the literature; however, if the leading term is absent there is a serious problem. Thus a meaningful phenomenology requires the inclusion of the LO RG effects. Doing so, the renormalization scale μ in [11] becomes the scale of new physics, and the results in that paper would correspond to $\mu_\Lambda = 1$ TeV.¹³

Next we would like to mention the analysis in [27]. RG Yukawa effects have been studied in a NP scenario in which the only operators with non-vanishing coefficients at μ_Λ are the third-generation (in the interaction basis) semi-leptonic four-fermion operators

¹³ Meanwhile the authors of [11] replaced the scale μ by μ_Λ so that their final formula agrees with ours. However, we disagree with their statement that μ_Λ comes from the diagram (c) in Fig. 1 as it is absent in this diagram and can only come from LO RG effects as explained above.

$\mathcal{O}_{\ell q}^{(1)} = (\bar{\ell}_L \gamma_\mu \ell_L)(\bar{q}_L \gamma^\mu q_L)$ and $\mathcal{O}_{\ell q}^{(3)} = (\bar{\ell}_L \gamma_\mu \sigma^a \ell_L)(\bar{q}_L \gamma^\mu \sigma^a q_L)$ of the Warsaw basis [6]. This structure has been motivated by the B -physics anomalies and can be met in models with vector leptoquark mediators. It has been demonstrated that RG Yukawa effects modify significantly the Z couplings to leptons, ruling out a possible explanation of the anomalies within this scenario because of the strong constraints from Z -pole observables and lepton-flavour violating τ decays. In our models these couplings are absent and are not generated by the RG Yukawa effects from the operators in (3) and (4) considered by us.

Finally, in [28] the impact of RH charged currents on ε'/ε in correlation with electric dipole moments (EDMs) has been analysed, considering the operator \mathcal{O}_{Hud} in (5). The phenomenology of this model is very different from the one of our models as the main mediators are W^\pm with RH couplings and not the Z boson. In this model contributions to ε_K are much smaller than in our models and it appears that it is harder to explain the ε'/ε anomaly when other constraints, in particular from EDMs, are taken into account. But the correlation of ε'/ε with EDMs pointed out in this paper is clearly interesting.

6 Implications for Flavour Observables

The matching and RG evolution in our setup is schematically shown in Fig. 4. The darker nodes are included in the following phenomenological analysis, while the lighter ones are contributions we do not consider here, but that would appear in a general SMEFT analysis. Solid lines represent direct matching and running contributions, while dashed lines are the main contributions created via RG effects, either via Yukawa couplings ($\sim y_t^2$) or via QCD ($\sim \alpha_s$). Note that in some cases these contributions can result in larger observable effects than the direct ones, due to RG and chiral enhancement factors, *e.g.* in the case of $\mathcal{O}_{LR,1}$. The dotted lines represent NLO matching effects.

The inclusion of new contributions from Yukawa RG evolution and the NLO corrections calculated here have only direct impact on $\Delta F = 2$ observables. However, in a combined phenomenological analysis of $\Delta F = 1, 2$ processes $\Delta F = 2$ observables will restrict the available parameter space and hence affect also predictions for $\Delta F = 1$ processes, specifically for RH couplings of the Z . In the present paper we want to illustrate this impact mainly in the latter case, as in this scenario the impact is very large.

Concentrating on RH couplings of the Z , we will first consider the correlation between the ratio ε'/ε , ε_K , $K_L \rightarrow \mu^+ \mu^-$ and $K \rightarrow \pi \nu \bar{\nu}$ decays analyzed in [10], where the contributions in question have not been taken into account. Subsequently we will consider the impact on the correlation between $B_{s,d}^0 - \bar{B}_{s,d}^0$ observables and rare $b \rightarrow d, s + (\ell^+ \ell^-, \nu \bar{\nu})$ decays.

The experimental data and hadronic inputs are identical to [14] with the exception that we include very recent preliminary data for $B_{d,s} \rightarrow \mu^+ \mu^-$ [29], combined with previous measurements in [30].

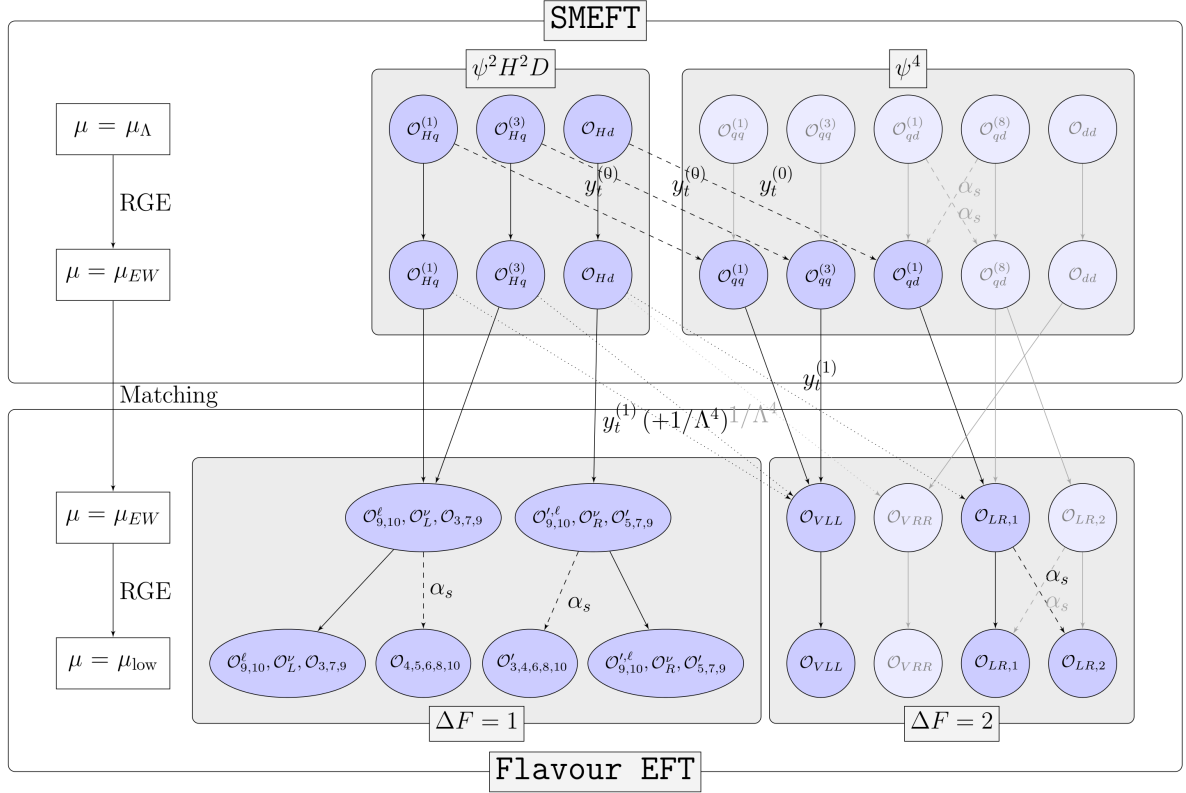


Figure 4: Visualization of matching and RG running for the operators under consideration in SMEFT and the $\Delta F = 1, 2$ -EFTs. The darker nodes are those that are dominant within our approach. Solid lines indicate $\mathcal{O}(1)$ running/matching contributions, dashed lines RG mixing enhanced by a large logarithm and dotted lines NLO running/matching contributions. Contributions via 1stLLA top-Yukawa RG mixing are denoted by $y_t^{(0)}$, 1-loop corrections to the matching at μ_{EW} by $y_t^{(1)}$. $1/\Lambda^4$ refers to contributions that appear at dimension eight, like double insertions of dim-6 operators.

6.1 Numerical impact on M_{12}

The off-diagonal element of the mass matrix of neutral meson mixing including the full set of $\Delta F = 2$ operators (16) is given by

$$M_{12}^{ij*} = \frac{\langle \bar{M}^0 | \mathcal{H}_{\Delta F=2}^{ij} | M^0 \rangle}{2M_{M^0}} = \frac{G_F^2 M_W^2}{8\pi^2 M_{M^0}} (\lambda_t^{ij})^2 \sum_a C_a^{ij}(\mu_{\text{low}}) \langle \bar{M}^0 | O_a^{ij} | M^0 \rangle(\mu_{\text{low}}) \quad (56)$$

in terms of Wilson coefficients and hadronic matrix elements of the operators, $\langle O_a^{ij} \rangle \equiv \langle \bar{M}^0 | O_a^{ij} | M^0 \rangle$, evaluated at the scale μ_{low} relevant for the corresponding meson system $ij = sd, bd, bs$. The hadronic matrix elements are provided by lattice collaborations, who for historical reasons relate them usually to bag-factors, thereby introducing additional dependences on the meson decay constant F_M and the chirality-factor

$$r_\chi^{ij} = \left[\frac{M_M}{m_i(\mu_{\text{low}}) + m_j(\mu_{\text{low}})} \right]^2 \quad (57)$$

that involves the $\overline{\text{MS}}$ quark masses.

The NP contributions of FC quark couplings of the Z in SMEFT require to consider the operators $a = \text{VLL}, \text{LR1}, \text{LR2}$, where $C_{\text{LR},2}$ enters via QCD RG evolution.¹⁴ For the Kaon system, we adapt the results of bag factors from RBC-UKQCD [31]. For the $B_{d,s}$ systems, we use the products of decay constants and bag factors, $F_{B_j}^2 B_a^{ij}$, from FNAL/MILC [32]. Both sets of coefficients are tabulated in Table 2. The relations between bag factors and matrix elements at μ_{low} for the choice of operator basis by RBC-UKQCD [31] are

$$\langle O_{\text{VLL}}^{sd} \rangle = \frac{2}{3} M_K^2 F_K^2 B_1^{sd}, \quad \langle O_a^{sd} \rangle = N_a^{sd} r_\chi^{sd} M_K^2 F_K^2 B_a^{sd}, \quad (58)$$

with $N_a^{sd} = (-1/3, 1/2)$ for $a = (\text{LR1}, \text{LR2})$, and for FNAL/MILC [32]

$$\langle O_{\text{VLL}}^{bj} \rangle = \frac{2}{3} M_{B_j}^2 F_{B_j}^2 B_1^{bj}, \quad \langle O_a^{bj} \rangle = N_a^{bj} (r_\chi^{bj} + d_a^{bj}) M_{B_j}^2 F_{B_j}^2 B_a^{bj}, \quad (59)$$

with $N_a^{bj} = (-1/3, 1/2)$ and $d_a^{bj} = (3/2, 1/6)$.

In order to illustrate the RG and chiral enhancement of NP contributions in $\Delta C_{\text{LR},1}$ (35) compared to ΔC_{VLL} (36), we express in M_{12}^{ij} the $C_i(\mu_{\text{low}})$ in terms of the $C_i(\mu_{\text{ew}})$, using QCD RG evolution at NLO [21, 33]. We keep the hadronic input unevaluated and use $\mu_{\text{ew}} \approx 163$ GeV in order to be able to adapt the SM calculations of M_{12}^{sd} at NNLO [34–36] and of M_{12}^{bj} at NLO. The semi-numerical result in terms of $C_i(\mu_{\text{ew}})$ is

$$\frac{M_{12}^{sd*}}{\mathcal{F}_{sd}} = \left[168.7 + i 194.1 + 0.8 \Delta C_{\text{VLL}}^{sd} \right] B_1^{sd} - \Delta C_{\text{LR},1}^{sd} (25.9 B_4^{sd} + 14.1 B_5^{sd}), \quad (60)$$

$$\frac{M_{12}^{bj*}}{\tilde{\mathcal{F}}_{bj}} = \left[1.95 + 0.84 \Delta C_{\text{VLL}}^{bj} \right] F_{B_j}^2 B_1^{bj} - \Delta C_{\text{LR},1}^{bj} F_{B_j}^2 (1.18 B_4^{bj} + 1.42 B_5^{bj}). \quad (61)$$

¹⁴Note that C_{VRR} can be included by $C_{\text{VLL}} \rightarrow C_{\text{VLL}} + C_{\text{VRR}}$.

ij	μ_{low} [GeV]	N_f	r_χ	B_1^{ij}	B_4^{ij}	B_5^{ij}
sd	3.0	3	30.8	0.525(16)	0.920(20)	0.707(45)
				$F_{B_j}^2 B_1^{ij}$	$F_{B_j}^2 B_4^{ij}$	$F_{B_j}^2 B_5^{ij}$
bd	4.18	5	1.6	0.0342(30)	0.0390(29)	0.0361(36)
bs	4.18	5	1.6	0.0498(32)	0.0534(32)	0.0493(37)

Table 2: Scale settings and number of flavours, N_f , as well as numerical inputs of bag factors entering M_{12}^{ij} , see [32] and [31] for correlations. For the Kaon system threshold crossings to $N_f = 4$ and $N_f = 3$ have been chosen as 4.18 GeV and 1.4 GeV.

The SM contribution is given by the first numbers in brackets $\propto B_1$ and the normalization factors read

$$\mathcal{F}_{ij} = \tilde{\mathcal{F}}_{ij} F_M^2 = \frac{G_F^2 M_W^2}{12 \pi^2} (\lambda_t^{ij})^2 M_M F_M^2. \quad (62)$$

The huge enhancement of $\Delta C_{\text{LR},1}^{sd}$ w.r.t. $\Delta C_{\text{VLL}}^{sd}$ in Kaon mixing stems in large part from r_χ^{sd} , whereas the effect is a factor of three in B -meson mixing. The SMEFT contributions (35) and (36) can be inserted into both equations to obtain numerical predictions for M_{12}^{ij} . There are two experimental constraints in each sector on M_{12}^{ij} ,

$$ij = sd : \quad \Delta M_K = 2 \text{Re} (M_{12}^{sd}), \quad \varepsilon_K \propto \text{Im} (M_{12}^{sd}), \quad (63)$$

$$ij = bj : \quad \Delta M_{B_j} = 2 |M_{12}^{bj}|, \quad \phi_j = \text{Arg} (M_{12}^{bj}), \quad (64)$$

where we have assumed that SM QCD penguin pollution and new physics in $b \rightarrow sc\bar{c}$ processes are negligible, see [37–40] for recent works.

6.2 Semileptonic $\Delta F = 1$ Processes

The $\Delta F = 1$ semileptonic processes $d_j \rightarrow d_i + (\ell^+ \ell^-, \nu \bar{\nu})$ are highly sensitive to FC quark couplings of the Z . The $\psi^2 H^2 D$ operators modify them at tree-level via Fig. 3a in SMEFT. The relevant parts of the $\Delta F = 1$ -EFTs,

$$\mathcal{H} = -\frac{4G_F}{\sqrt{2}} \lambda_t^{ij} \frac{\alpha_e}{4\pi} \sum_a C_a^{ij} O_a^{ij}, \quad (65)$$

involve the six semileptonic operators

$$O_{9(9')}^{ij} = [\bar{d}_i \gamma_\mu P_{L(R)} d_j] [\bar{\ell} \gamma^\mu \ell], \quad O_{10(10')}^{ij} = [\bar{d}_i \gamma_\mu P_{L(R)} d_j] [\bar{\ell} \gamma^\mu \gamma_5 \ell], \quad (66)$$

$$O_{L(R)}^{ij} = [\bar{d}_i \gamma_\mu P_{L(R)} d_j] [\bar{\nu} \gamma^\mu (1 - \gamma_5) \nu]. \quad (67)$$

The Wilson coefficients of the LH operators at μ_{ew} read as follows [41, 42]:

$$C_9^{ij} = \frac{Y(x_t)}{s_W^2} - 4Z(x_t) - \frac{\pi}{\alpha_e} \frac{v^2}{\lambda_t^{ij}} (1 - 4s_W^2) [\mathcal{C}_{Hq}^{(1)} + \mathcal{C}_{Hq}^{(3)}]_{ij} + \dots, \quad (68)$$

$$C_{10}^{ij} = -\frac{Y(x_t)}{s_W^2} + \frac{\pi}{\alpha_e} \frac{v^2}{\lambda_t^{ij}} [\mathcal{C}_{Hq}^{(1)} + \mathcal{C}_{Hq}^{(3)}]_{ij} + \dots, \quad (69)$$

$$C_L^{ij} = -\frac{X(x_t)}{s_W^2} + \frac{\pi}{\alpha_e} \frac{v^2}{\lambda_t^{ij}} [\mathcal{C}_{Hq}^{(1)} + \mathcal{C}_{Hq}^{(3)}]_{ij} + \dots, \quad (70)$$

where the SM contributions are given by the gauge-independent functions $X(x_t)$, $Y(x_t)$ and $Z(x_t)$ [3]. The tree-level matching of SMEFT gives rise to the dependence on the sum $\mathcal{C}_{Hq}^{(1)} + \mathcal{C}_{Hq}^{(3)}$ and the dots indicate potential additional contributions, for instance from ψ^4 operators. The chirality-flipped Wilson coefficients

$$C_{9'}^{ij} = -(1 - 4s_W^2) \frac{\pi}{\alpha_e} \frac{v^2}{\lambda_t^{ij}} [\mathcal{C}_{Hd}]_{ij} + \dots, \quad C_{10'}^{ij} = \frac{\pi}{\alpha_e} \frac{v^2}{\lambda_t^{ij}} [\mathcal{C}_{Hd}]_{ij} + \dots, \quad (71)$$

$$C_R^{ij} = \frac{\pi}{\alpha_e} \frac{v^2}{\lambda_t^{ij}} [\mathcal{C}_{Hd}]_{ij} + \dots, \quad (72)$$

depend on \mathcal{C}_{Hd} . $C_{9,9'}$ depend on the same combination of coefficients $\mathcal{C}_{\psi^2 H^2 D}$ as $C_{10,10'}$, but with an additional suppression factor $1 - 4s_W^2 \approx 0.08$. There is also a strict relation $C_{10'}^{ij} = C_R^{ij}$, which holds equivalently for the NP parts of C_{10} and C_L . Therefore all semileptonic $\Delta F = 1$ processes depend on only one left-handed and one right-handed combination of Wilson coefficients.

Whenever only one of these combinations is present, strong correlations are present in each sector $ij = sd, bd, bs$. For instance the semileptonic decays with neutrinos and a pseudoscalar meson in the final state, *e.g.* $K^+ \rightarrow \pi^+ \nu \bar{\nu}$, $K_L \rightarrow \pi^0 \nu \bar{\nu}$, $B \rightarrow K \nu \bar{\nu}$ and the leptonic decays $M_{ij} \rightarrow \ell^+ \ell^-$ ($K_L \rightarrow \mu^+ \mu^-$, $B_q \rightarrow \ell^+ \ell^-$) depend only on $C_{10,10'}$ and $C_{L,R}$, respectively. The dependence of the corresponding branching ratios on $\mathcal{C}_{\psi^2 H^2 D}$ Wilson coefficients reads

$$\text{Br}(M_j \rightarrow P_i \nu \bar{\nu}) \propto \left| -\frac{X(x_t)}{s_W^2} + \frac{\pi}{\alpha_e} \frac{v^2}{\lambda_t^{ij}} [\mathcal{C}_{Hq}^{(1)} + \mathcal{C}_{Hq}^{(3)} + \mathcal{C}_{Hd}]_{ij} \right|^2, \quad (73)$$

$$\text{Br}(M_{ij} \rightarrow \ell^+ \ell^-) \propto \left| -\frac{Y(x_t)}{s_W^2} + \frac{\pi}{\alpha_e} \frac{v^2}{\lambda_t^{ij}} [\mathcal{C}_{Hq}^{(1)} + \mathcal{C}_{Hq}^{(3)} - \mathcal{C}_{Hd}]_{ij} \right|^2. \quad (74)$$

These observables are clearly correlated if only LH or RH couplings are present, but are independent as soon as both couplings are finite. The full set of semileptonic decays $d_j \rightarrow d_i + (\ell^+ \ell^-, \nu \bar{\nu})$ includes further observables that depend also on $C_{9,9'}$, and allow to put further constraints on these Wilson coefficients.

Additional correlations exist between $\Delta F = 1$ and $\Delta F = 2$ processes, at least for the RH scenario, which will be discussed in the next section.

6.3 Correlations between $\Delta F = 2$ and $\Delta F = 1$ Processes

The dependence on \mathcal{C}_{Hd} of the $\Delta F = 2$ contribution (35) implies a strong correlation of the aforementioned semileptonic decays with M_{12}^{ij} for RH interactions, to be discussed below. As already mentioned in Section 5, such a correlation is not present for NP LH Z couplings. This is due to the presence of two Wilson coefficients, conveniently written as the combinations

$$\mathcal{C}_{Hq}^{(\pm)} \equiv \mathcal{C}_{Hq}^{(1)} \pm \mathcal{C}_{Hq}^{(3)}, \quad (75)$$

which appear in different combinations in $\Delta F = 1$ and $\Delta F = 2$: $\Delta F = 1$ processes depend only on $\mathcal{C}_{Hq}^{(+)}$, whereas $\Delta F = 2$ processes depend on $\mathcal{C}_{Hq}^{(-)}$ when restricting to the 1stLLA term. As can be seen from (36), the latter changes once the NLO corrections are included:

$$\begin{aligned} \Delta C_{\text{VLL}}^{ij}(\mu_{\text{ew}}) &= \frac{v^2}{\lambda_t^{ij}} x_t \left[[\mathcal{C}_{Hq}^{(-)}]_{ij} \left(\ln \frac{\mu_\Lambda}{M_W} + \begin{Bmatrix} 0.6 \\ 1.2 \end{Bmatrix} \right) - [\mathcal{C}_{Hq}^{(+)}]_{ij} \begin{Bmatrix} 1.3 \\ 1.9 \end{Bmatrix} \right] \\ &= \frac{v^2}{\lambda_t^{ij}} x_t \left[[\mathcal{C}_{Hq}^{(-)}]_{ij} \begin{Bmatrix} 5.4 \\ 6.0 \end{Bmatrix} - [\mathcal{C}_{Hq}^{(+)}]_{ij} \begin{Bmatrix} 1.3 \\ 1.9 \end{Bmatrix} \right] \quad \text{for} \quad \begin{cases} ij = bd, bs \\ ij = sd \end{cases}. \end{aligned} \quad (76)$$

Here we have used $\mu_\Lambda = 10$ TeV and numerical results presented in Section 4.2 for $H_1(x_t, M_W) = -0.7$, $H_2(x_t, M_W) = +3.0$ and (43) for $ij = bd, bs$. The dependence of $\Delta F = 2$ on $\mathcal{C}_{Hq}^{(+)}$ is by about a factor three weaker compared to one of $\mathcal{C}_{Hq}^{(-)}$. Despite the presence of $\mathcal{C}_{Hq}^{(+)}$, $\Delta F = 2$ constraints will not constrain $\Delta F = 1$ observables, as long as the $\mathcal{C}_{Hq}^{(\pm)}$ are arbitrary. However, in specific models they can be related, yielding again correlations. The influence of $\Delta F = 2$ remains weaker than in the RH case though, given the absence of chiral and RG enhancements.

In addition to $\Delta F = 2$ and semileptonic $\Delta F = 1$ processes we consider in the Kaon sector also one non-leptonic $\Delta F = 1$ observable, namely ε'/ε . We parameterize NP effects in this quantity as [10]

$$\frac{\varepsilon'}{\varepsilon} = \left(\frac{\varepsilon'}{\varepsilon} \right)^{\text{SM}} + \left(\frac{\varepsilon'}{\varepsilon} \right)^{\text{NP}} = \left(\frac{\varepsilon'}{\varepsilon} \right)^{\text{SM}} + \kappa_{\varepsilon'} \cdot 10^{-3} \quad (77)$$

and use the expressions given in [14] to express $\kappa_{\varepsilon'}$ as a linear function of $[\mathcal{C}_{Hd}]_{sd}$ and $[\mathcal{C}_{Hq}^{(+)}]_{sd}$, see also [10]. These expressions are unaffected by the new contributions calculated in this work. As in [14] we use the very conservative bound $\kappa_{\varepsilon'} \in [0, 2]$, reflecting the fact that the experimental world average from the NA48 [43] and KTeV [44, 45] collaborations,

$$(\varepsilon'/\varepsilon)_{\text{exp}} = (16.6 \pm 2.3) \times 10^{-4}, \quad (78)$$

is larger than recent theoretical estimates [46–51].

6.3.1 Correlations for RH Z couplings

We start by assuming the presence of only RH NP Z couplings, *i.e.* $\mathcal{C}_{Hd} \neq 0$. In this case, in principle two observables per sector $ij = sd, bd, bs$ are sufficient to determine both real

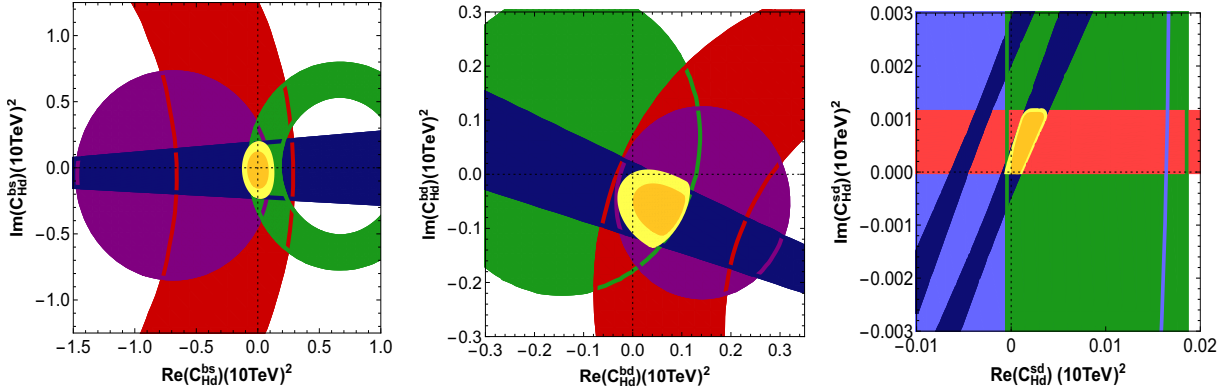


Figure 5: Constraints on the couplings $[\mathcal{C}_{Hd}]_{ij}$ from $b \rightarrow s$ (left), $b \rightarrow d$ (middle) and $s \rightarrow d$ (right) observables at $\mu_\Lambda = 10$ TeV, assuming these are the only couplings present at μ_Λ . The constraints shown correspond to the observables Δm_s (dark red), ϕ_s (dark blue), $\text{Br}(B_s \rightarrow \mu^+ \mu^-)$ (green) and $\text{Br}(B^+ \rightarrow K^+ \mu^+ \mu^-)_{[15,22]}$ (purple) for $b \rightarrow s$, to Δm_d (dark red), $\sin 2\beta$ (dark blue), $\text{Br}(B_d \rightarrow \mu^+ \mu^-)$ (green) and $\text{Br}(B^+ \rightarrow \pi^+ \mu^+ \mu^-)_{[15,22]}$ (purple) for $b \rightarrow d$, and ε_K (dark blue), ϵ'/ϵ (light red), $\text{Br}(K^+ \rightarrow \pi^+ \nu \bar{\nu})$ (light blue) and $\text{Br}(K_L \rightarrow \mu^+ \mu^-)$ (green) for $s \rightarrow d$ transitions. The global fit to each sector is shown in yellow. All coloured areas correspond to 95% CL, only the dark yellow area to 68%.

and imaginary part of this coefficient. The fits for the three sectors are shown in Fig. 5. We have chosen $\mu_\Lambda = 10$ TeV in order to guarantee sufficient suppression of potential dimension eight contributions as explained in Section 5. In all three sectors a consistent combined fit is possible, restricting \mathcal{C}_{Hd} to lie in a range close to the SM point $\mathcal{C}_{Hd} = 0$: the obtained ranges are

$$|\mathcal{C}_{Hd}^{bs}| \lesssim \frac{0.25}{(10 \text{ TeV})^2}, \quad |\mathcal{C}_{Hd}^{bd}| \lesssim \frac{0.15}{(10 \text{ TeV})^2}, \quad |\mathcal{C}_{Hd}^{sd}| \lesssim \frac{0.004}{(10 \text{ TeV})^2}. \quad (79)$$

The hierarchy in these results follows roughly that of the corresponding CKM combinations λ_{ij}^t . It is seen how the combined fit is determined in all three sectors by observables from both $\Delta F = 1$ and $\Delta F = 2$: ϕ_s , $\text{Br}(B^+ \rightarrow K^+ \mu^+ \mu^-)$ and $\text{Br}(B_s \rightarrow \mu^+ \mu^-)$ for $b \rightarrow s$, $\sin 2\beta$, $\text{Br}(B^+ \rightarrow \pi^+ \mu^+ \mu^-)$ and $\text{Br}(B_d \rightarrow \mu^+ \mu^-)$ for $b \rightarrow d$, and ε_K , ϵ'/ϵ , $K^+ \rightarrow \pi^+ \nu \bar{\nu}$ and $\text{Br}(K_L \rightarrow \mu^+ \mu^-)$ in $s \rightarrow d$. The increased importance of $\Delta F = 2$ observables in this context compared to earlier works is due to the new contributions calculated above. Especially ε_K , fully dominated by the new contribution from $O_{\text{LR},1}$, is now the most constraining observable for $s \rightarrow d$ together with ϵ'/ϵ .

To illustrate the influence of $\Delta F = 2$ observables further, we show in Fig. 6 the resulting correlations between observables in the Kaon sector with and without taking the $\Delta F = 2$ constraint from ε_K into account. Taking only $\Delta F = 1$ into account, in many cases the present upper limits for observables like $\text{Br}(K^+ \rightarrow \pi^+ \nu \bar{\nu})$ can be reached, *i.e.* enhancements compared to the SM of up to a factor 5. On the other hand, the resulting predictions for rare decays when including $\Delta F = 2$ are rather close to the SM; specifically, $\text{Br}(K^+ \rightarrow \pi^+ \nu \bar{\nu})$ is predicted to be enhanced, but only up to 50% of the SM value.

In contrast to $s \rightarrow d$, we show in Fig. 7 correlations with and without $\Delta F = 1$ constraints for $b \rightarrow s$ transitions. Since from Fig. 5 it can be seen that $\Delta F = 1$ dominate the global fit, it does not surprise that the allowed ranges again become much larger

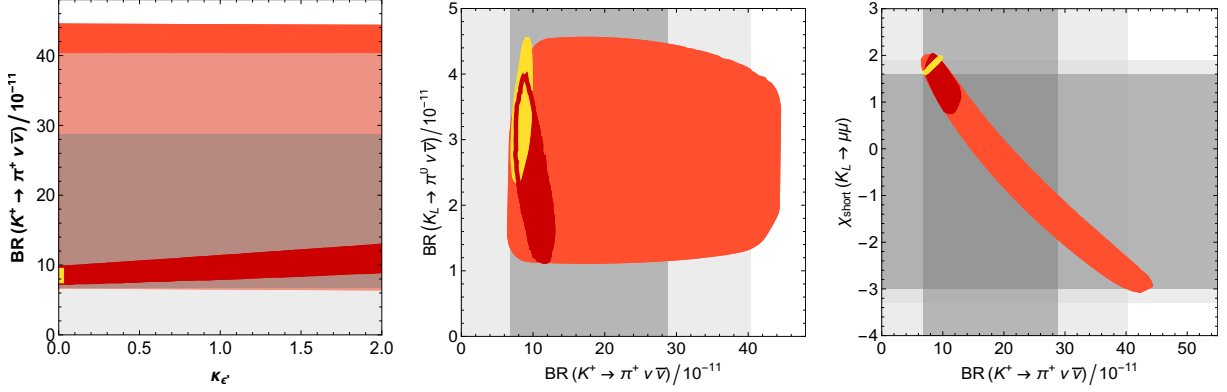


Figure 6: Correlations between $s \rightarrow d$ observables and $\kappa_{e'}$ in the presence of right-handed NP FC Z couplings, only, including (darker colours) and excluding (lighter colours) constraints from $\Delta F = 2$: $\text{Br}(K^+ \rightarrow \pi^+ \nu \bar{\nu})$ vs. $\kappa_{e'}$ (left), $\text{Br}(K_L \rightarrow \pi^0 \nu \bar{\nu})$ vs. $\text{Br}(K^+ \rightarrow \pi^+ \nu \bar{\nu})$ (middle), and $\chi_{\text{short}}(K_L \rightarrow \mu^+ \mu^-)$ vs. $\text{Br}(K^+ \rightarrow \pi^+ \nu \bar{\nu})$ (right). All coloured areas correspond to 95% CL, the yellow areas are the SM predictions. The dark and light grey areas indicate the 1- and 2 σ experimental ranges.

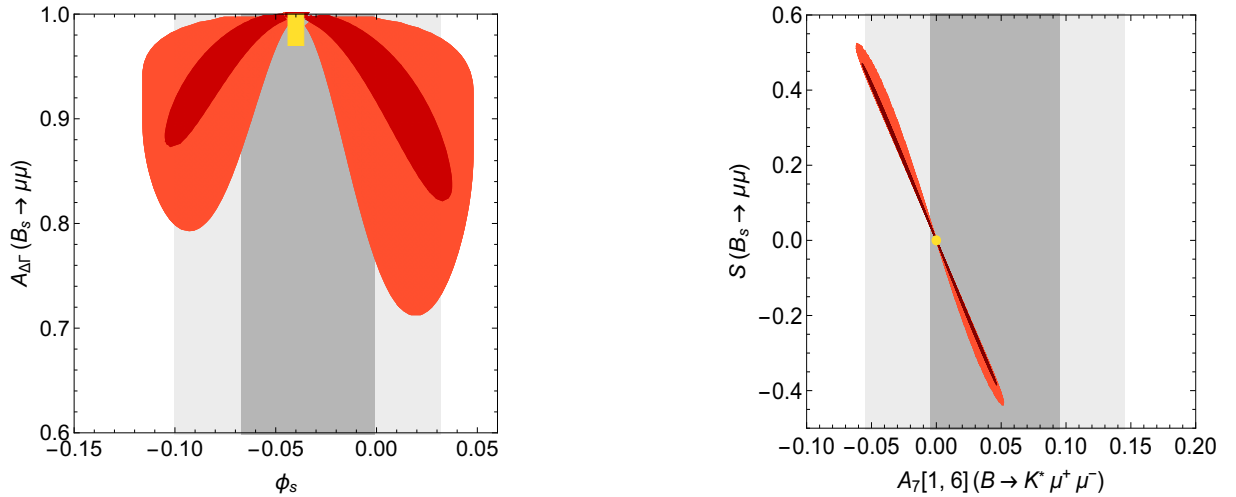


Figure 7: Correlations between $b \rightarrow s$ observables in the presence of right-handed NP FC Z couplings, only, including (darker colours) and excluding (lighter colours) constraints from $\Delta F = 1$: $A_{\Delta\Gamma}(B_s \rightarrow \mu^+ \mu^-)$ vs. ϕ_s (left) and $S(B_s \rightarrow \mu^+ \mu^-)$ vs. $A_7[1,6](B \rightarrow K^* \mu^+ \mu^-)$ (right). All coloured areas correspond to 95% CL, the yellow areas are the SM predictions. The dark and light grey areas indicate the 1- and 2 σ experimental ranges.

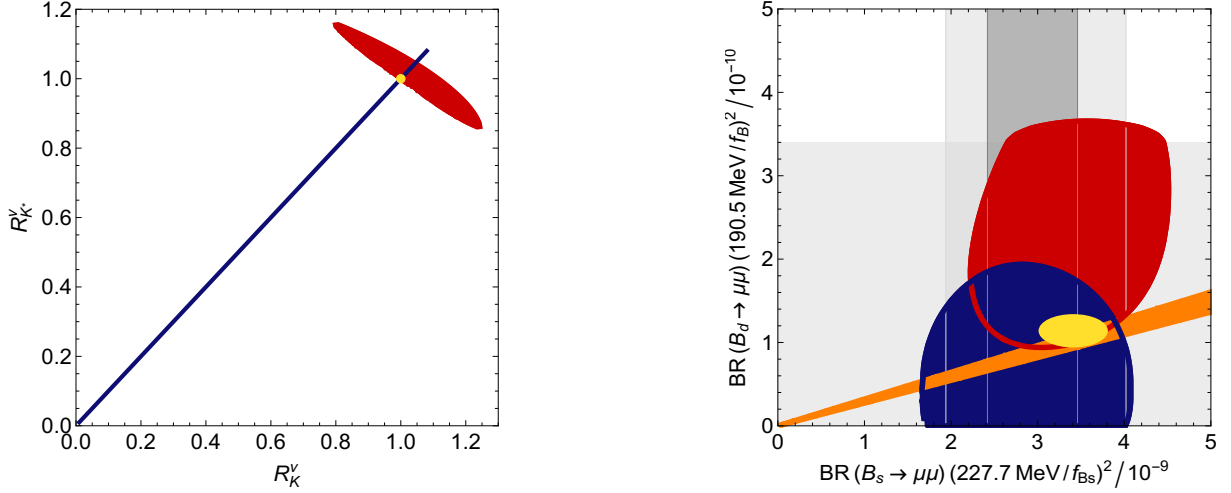


Figure 8: Correlations between $R_K^{\nu*}$ vs. R_K^{ν} (left) and $\text{Br}(B_d \rightarrow \mu^+\mu^-)$ vs. $\text{Br}(B_s \rightarrow \mu^+\mu^-)$ (right) in purely LH (blue) or RH (red) scenarios. All coloured areas correspond to 95% CL, the yellow areas are the SM predictions. The dark and light grey areas indicate the 1- and 2 σ experimental ranges. The orange band in the right plot corresponds to a scenario of constrained minimal flavour violation (CMFV) [42].

when excluding the corresponding observables; clearly only the combination of $\Delta F = 1$ and $\Delta F = 2$ constraints paints the full picture. There is a strong correlation in the RH scenario between the mass-eigenstate rate asymmetry $A_{\Delta\Gamma}(B_s \rightarrow \mu^+\mu^-)$ and ϕ_s that can be tested in the near future at LHCb. We show also the strong correlation between the mixing-induced CP asymmetry $S(B_s \rightarrow \mu^+\mu^-)$ and one of the T-odd CP asymmetries in $B \rightarrow K^*\mu^+\mu^-$, where apart from the shown A_7 , also A_8 and A_9 are subject of improving measurements at LHCb. Note that to very high accuracy $(A_{\Delta\Gamma})^2 + (S)^2 = 1$ in $B_s \rightarrow \mu^+\mu^-$ due to a vanishing direct CP-asymmetry. In RH scenarios there is also a strong correlation between $A_{7,8,9}$.

Finally, in Fig. 8 we directly compare models with only RH and only LH NP Z couplings by showing the correlations between R_K^{ν} and $R_K^{\nu*}$ [42],

$$R_{K^{(*)}}^{\nu} = \frac{\text{Br}(B \rightarrow K^{(*)}\nu\bar{\nu})}{\text{Br}(B \rightarrow K^{(*)}\nu\bar{\nu})|_{\text{SM}}}, \quad (80)$$

as well as $\text{Br}(B_s \rightarrow \mu^+\mu^-)$ and $\text{Br}(B_d \rightarrow \mu^+\mu^-)$. For RH models, shown in dark red, we observe a strong anti-correlation between the two modes with neutrinos in the final state, each allowed to deviate up to $\sim 20\%$ from its SM value. Furthermore, $\text{Br}(B_s \rightarrow \mu^+\mu^-)$ is slightly pulled to larger values by $\text{Br}(B^+ \rightarrow K^+\mu^+\mu^-)$, see Fig. 5, and $\text{Br}(B_d \rightarrow \mu^+\mu^-)$ is predicted to be at least as large as the SM value, with values allowed up to the present experimental upper limit; lower values are in tension with $\text{Br}(B^+ \rightarrow \pi^+\mu^+\mu^-)$ as well as Δm_d , see again Fig. 5.

6.3.2 Correlations for LH Z couplings

Making the assumption that only LH NP couplings of the Z are non-vanishing, $\mathcal{C}_{Hq}^{(1,3)} \neq 0$, changes the picture qualitatively. For each sector there are now two complex coefficients;

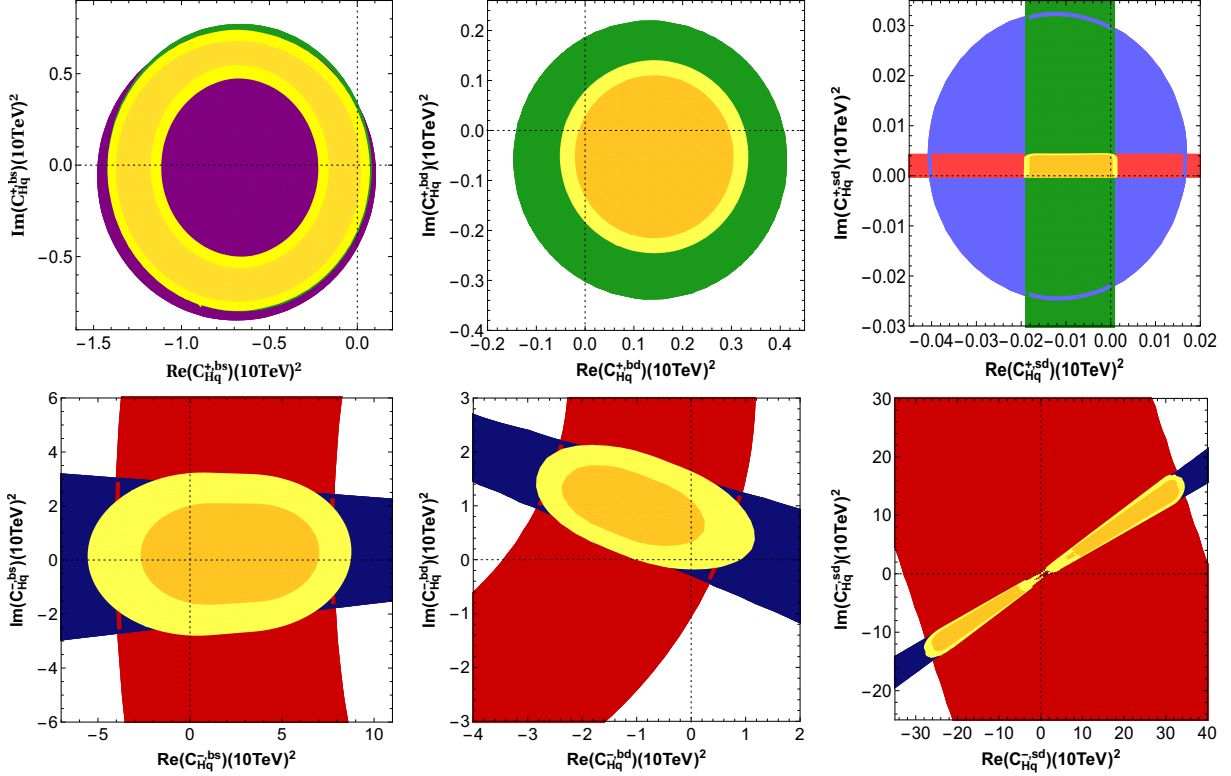


Figure 9: Constraints on the couplings $[\mathcal{C}_{Hq}^{(\pm)}]_{ij}$ from $b \rightarrow s$ (left), $b \rightarrow d$ (middle) and $s \rightarrow d$ (right) observables at $\mu_\Lambda = 10$ TeV, assuming these are the only couplings present at μ_Λ . The $\Delta F = 2$ constraints shown in the $[\mathcal{C}_{Hq}^{(-)}]_{ij}$ planes in the lower row are at LO. The constraints shown correspond to the observables Δm_s (dark red), ϕ_s (dark blue), $\text{Br}(B_s \rightarrow \mu^+ \mu^-)$ (green) and $\text{Br}(B^+ \rightarrow K^+ \mu^+ \mu^-)_{[15,22]}$ (purple) for $b \rightarrow s$, to Δm_d (dark red), $\sin 2\beta$ (dark blue), $\text{Br}(B_d \rightarrow \mu^+ \mu^-)$ (green) and $\text{Br}(B^+ \rightarrow \pi^+ \mu^+ \mu^-)_{[15,22]}$ (purple) for $b \rightarrow d$, and ε_K (dark blue), ε'/ε (light red), $\text{Br}(K^+ \rightarrow \pi^+ \nu \bar{\nu})$ (light blue) and $\text{Br}(K_L \rightarrow \mu^+ \mu^-)$ (green) for $s \rightarrow d$ transitions. The global fit to each sector is shown in yellow. All coloured areas correspond to 95% CL, only the dark yellow area to 68%.

in order to obtain plots similar to Fig. 5, we show in Fig. 9 the constraints from $\Delta F = 1$ in the $\mathcal{C}_{Hq}^{(+)}$ plane and from $\Delta F = 2$ in the $\mathcal{C}_{Hq}^{(-)}$ plane; the latter constraints are shown at LO, *i.e.* based on (29) and (30), to have only this coefficient appear. These coefficients are both much weaker constrained than in the RH case. The reasons for that are not only the absence of chiral and RG enhancements for LH contributions and the presence of two coefficients, but also the different interference pattern in $\Delta F = 1$: while for the RH the two main constraints intersect only in a small area, they essentially lie on top of each other for LH couplings. This is due to a relative sign for LH and RH contributions analogous to the one between (73) and (74). Finally, in the case of $[\mathcal{C}_{Hq}^{(-)}]_{sd}$ the fact that the long-distance contribution to Δm_K has large uncertainties renders this constraint extremely weak; here progress on the lattice is necessary to make this a useful constraint.

In order to demonstrate the influence of our NLO calculation, we show in Fig. 10 additionally the combined fits for $b \rightarrow d$ in the planes of the real- and imaginary parts of $\mathcal{C}_{Hq}^{(1,3)}$ at LO and NLO. At NLO the allowed regions shrink due to the larger coefficients

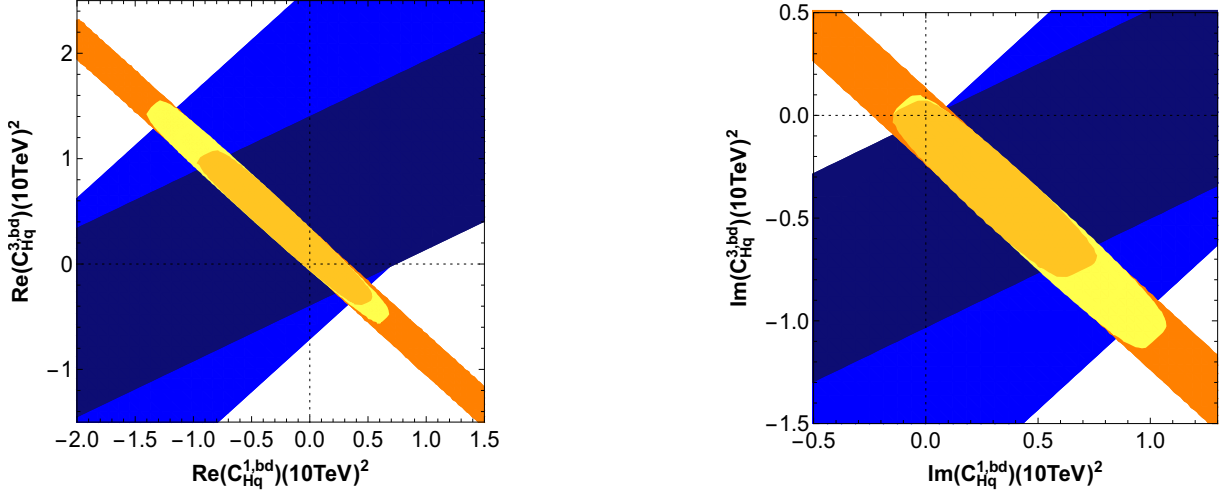


Figure 10: Constraints on the couplings $[\mathcal{C}_{Hq}^{(1,3)}]_{bd}$ at $\mu_\Lambda = 10$ TeV, assuming these are the only couplings present at μ_Λ . The combined $\Delta F = 1$ constraints are shown in orange, the $\Delta F = 2$ constraints at LO in blue and at NLO in dark blue. The combined fit is shown at LO in yellow and at NLO in dark yellow. All coloured areas correspond to 95% CL.

in (76); additionally the $\Delta F = 2$ constraint is rotated in the $\mathcal{C}_{Hq}^{(1)} - \mathcal{C}_{Hq}^{(3)}$ -plane, due to the additional contribution from $\mathcal{C}_{Hq}^{(+)}$, see (76).

While there are in general no correlations between $\Delta F = 1$ and $\Delta F = 2$, the ones within the $\Delta F = 1$ sector remain. We illustrate these correlations in Fig. 11. Importantly, we observe that also in this case no sizable enhancement of $\text{Br}(K^+ \rightarrow \pi^+ \nu \bar{\nu})$ is possible. This is related to our treatment of $K_L \rightarrow \mu^+ \mu^-$, which utilizes the approach [52] that derived bounds on the short-distance part χ_{SD} of its decay amplitude. Based on the quite general assumptions stated in [52, 53] the sign of the interference between long- and short-distance contributions can be predicted, leading to a stronger bound on the short-distance part, $-3.1 \leq \chi_{\text{SD}} \leq 1.7$, used in our fits. In Fig. 11 on the left we show the correlation between $\text{Br}(K^+ \rightarrow \pi^+ \nu \bar{\nu})$ and $\text{Br}(K_L \rightarrow \pi^0 \nu \bar{\nu})$ with (dark blue) and without (light blue) this assumption. Without this assumption positive values for the real part of $\mathcal{C}_{Hq}^{(+)}$ become allowed, which in turn allows for an enhancement of $\text{Br}(K^+ \rightarrow \pi^+ \nu \bar{\nu})$ of up to a factor of two compared to the SM, but still this branching ratio is in our scenarios stronger constrained from other modes than from the direct measurement. The correlation between ϵ'/ϵ and $\text{Br}(K_L \rightarrow \pi^0 \nu \bar{\nu})$, shown in the same figure on the right, is not affected by the assumption on $K_L \rightarrow \mu^+ \mu^-$, since these constraints are related to the imaginary part of $\mathcal{C}_{Hq}^{(+)}$, only. These observables are anti-correlated, so that a large value for $\kappa_{\epsilon'}$ would imply a strong suppression of $\text{Br}(K_L \rightarrow \pi^0 \nu \bar{\nu})$ [10, 54].

The correlations between R_K^ν and $R_{K^*}^\nu$ and between $\text{Br}(B_s \rightarrow \mu^+ \mu^-)$ and $\text{Br}(B_d \rightarrow \mu^+ \mu^-)$ allow to distinguish LH and RH scenarios for a large part of the parameter space, as shown in Fig. 8 (LH in dark blue): since in the LH scenario the interference with the SM is the same in $B \rightarrow K \nu \bar{\nu}$ and $B \rightarrow K^* \nu \bar{\nu}$, there is a very strict prediction $R_K^\nu/R_{K^*}^\nu \equiv 1$ [42]. An enhancement of each of the ratios is possible only up to $\sim 10\%$ in this scenario, but a strong suppression is possible, in contrast to RH models. For $\text{Br}(B_d \rightarrow \mu^+ \mu^-)$ a moderate enhancement up to $\sim 2 \times 10^{-10}$ is possible, but again a

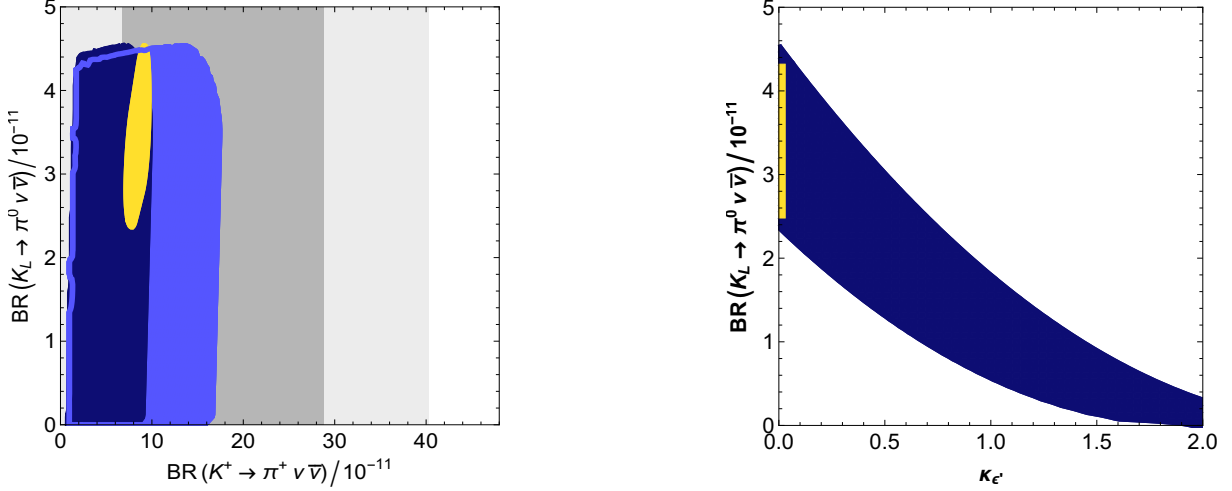


Figure 11: Correlations between $s \rightarrow d$ observables in the presence of left-handed NP FC Z couplings, only. $\text{BR}(K_L \rightarrow \pi^0 \nu \bar{\nu})$ vs. $\text{BR}(K^+ \rightarrow \pi^+ \nu \bar{\nu})$ (left) and $\text{BR}(K_L \rightarrow \pi^0 \nu \bar{\nu})$ vs. $\kappa_{\epsilon'}$ (right). The dark blue area in the left plot corresponds to using the assumption on the phase in $K_L \rightarrow \mu^+ \mu^-$, see text, the light blue area to not making this assumption. All coloured areas correspond to 95% CL, the yellow line is the SM prediction. The dark and light grey areas indicate the 1- and 2σ experimental ranges.

strong suppression, in contrast with the RH case.

7 Summary and Conclusions

In this paper we have addressed the Z -mediated contributions to $\Delta F = 2$ observables from the point of view of the SMEFT. Such an analysis goes beyond the simplified framework presented in [8], in which only pure BSM contributions involving two vertices generated by NP have been included and the Yukawa renormalization group effects not been taken into account. Once the latter effects are included at LO, their sizable unphysical scale dependence requires the calculation of NLO corrections. Both effects have been calculated in the present paper for the first time.

Among the new findings, listed as points 1.-5. in the Introduction, the most important is the generation of large LR operator contributions through RG Yukawa evolution in models with flavour-changing RH neutral currents. We have calculated these effects at LO using the results of [12].

At NLO we have addressed the contributions, pointed out recently in [11], in which one of the BSM vertices in Z exchange is replaced by the SM Z -penguin vertex. We have pointed out that the latter contributions are by themselves gauge dependent and, using SMEFT, calculated the remaining contributions that cancel this gauge dependence. This NLO calculation has significant impact on the original results presented in [11], where these contributions have not been included; however, the dominant new effect comes from the RG Yukawa evolution, which is included in this work for the first time. The comparison with the published version of [11] is given in Section 5.

In the course of our analysis we have found two new gauge-independent functions

$H_1(x_t)$ and $H_2(x_t)$, given in (37) and (38), respectively, that enter the phenomenology of these new contributions together with FC quark couplings of the Z generated by NP, given in (6), and the Yukawa RG effects mentioned above.

The impact of these new effects has been illustrated model-independently by considering the correlations between $\Delta F = 1$ and $\Delta F = 2$ observables in the down-quark sector. These are strongest in the presence of only RH NP Z couplings: the new effects strengthen the constraints from $\Delta F = 2$, especially in the Kaon sector. For instance, ε_K now restricts the coupling $[\mathcal{C}_{Hd}]_{sd}$ in such a way that only small enhancements of $\text{Br}(K^+ \rightarrow \pi^+ \nu \bar{\nu})$ remain allowed, about 50%. In the $b \rightarrow s$ sector and to less extent also in the $b \rightarrow d$ sector, $\Delta F = 1$ constraints remain dominant, but allow still for sizable NP contributions, *e.g.* in $B_{d,s} \rightarrow \mu^+ \mu^-$. In particular $B_d \rightarrow \mu^+ \mu^-$ can be enhanced to the present upper bound. Nevertheless, the strong correlations in this scenario will allow for distinguishing it from other NP models with coming data from the LHC (LHCb, CMS, ATLAS) and Belle II.

For NP models that yield only LH FC Z couplings, contributions to $\Delta F = 1$ and $\Delta F = 2$ are in general completely decoupled, since two Wilson coefficients are present – $\mathcal{C}_{Hq}^{(1)}$ and $\mathcal{C}_{Hq}^{(3)}$ – and enter in different combinations in $\Delta F = 1$ and $\Delta F = 2$. Furthermore the RG and chiral enhancements present for the RH $\Delta F = 2$ contributions are absent, such that large NP effects remain allowed in this sector, especially in Δm_K , where the SM prediction suffers from large long-distance effects. The correlations for $\Delta F = 1$ processes remain, however, since they are all sensitive to the same combination of Wilson coefficients, $\mathcal{C}_{Hq}^{(+)}$. We find that $\text{Br}(K^+ \rightarrow \pi^+ \nu \bar{\nu})$ is limited by its SM value in this case, which is related to our treatment of the constraint from $\text{Br}(K_L \rightarrow \mu^+ \mu^-)$ [52, 53]; should the corresponding assumptions be violated, an enhancement up to a factor of two w.r.t. the SM is possible, a bound that is still much stronger than the present experimental limit. Measuring a significant enhancement of this mode could therefore exclude both scenarios; this is also true for $\text{Br}(K_L \rightarrow \pi^0 \nu \bar{\nu})$ which can only be suppressed compared to its SM value, which is due to the constraint from ε'/ε , in accordance with [10].

In LH scenarios the $\text{SU}(2)_L$ invariance of SMEFT implies that the two Wilson coefficients $\mathcal{C}_{Hq}^{(1)}$ and $\mathcal{C}_{Hq}^{(3)}$ enter also up-type quark $\Delta F = 1$ FCNC processes with the same linear combination as in $\Delta F = 2$ down-type mixing. Therefore there are in principle also correlations among down-type $\Delta F = 2$ mixing and up-type $\Delta F = 1$ FCNC processes. They can be quite strong – see (10) – when certain conditions are met, *i.e.* the hierarchy of CKM elements remains as extracted in the SM and is not overcompensated by a hierarchy in $[\mathcal{C}_{Hq}^{(1,3)}]_{ij}$.

One of the important messages from our paper is that while ε'/ε can easily be enhanced in the LH and RH scenarios considered by us, $\text{Br}(K^+ \rightarrow \pi^+ \nu \bar{\nu})$ can only be suppressed (enhanced up to a factor of two) in the LH case if the stricter (conservative) bound on $K_L \rightarrow \mu \bar{\mu}$ is used and enhanced by at most 50% in the RH case. If the future results from the NA62 experiment will find much larger enhancement of $\text{Br}(K^+ \rightarrow \pi^+ \nu \bar{\nu})$ and later KOTO will also find an enhanced $\text{Br}(K_L \rightarrow \pi^0 \nu \bar{\nu})$, the only solution in the context of the Z scenario would be to consider the operators $\mathcal{O}_{Hq}^{(1)}$, $\mathcal{O}_{Hq}^{(3)}$ and \mathcal{O}_{Hd} simultaneously [10]. Alternatively other contributions, like the ones from four-fermion operators generated by Z' exchanges or exchanges of other heavy particles will be required.

Our analysis did not specify the origin of FC Z -boson couplings. The inclusion of these new effects in VLQ models in which concrete dynamics generates such couplings is

discussed in [14].

Acknowledgements

The research Ch.B, A.J.B and M.J was supported by the DFG cluster of excellence “Origin and Structure of the Universe”. The work of A.C. is supported by the Alexander von Humboldt Foundation. This work is also supported in part by the DFG SFB/TR 110 “Symmetries and the Emergence of Structure in QCD”.

A SMEFT

The covariant derivative in our conventions is

$$\mathcal{D}_\mu = \partial_\mu - ig_2 \frac{\sigma^a}{2} W_\mu^a - ig_1 Y B_\mu \quad (81)$$

with the $SU(2)_L$ and $U(1)_Y$ gauge couplings $g_{2,1}$ and σ^a denoting the Pauli matrices. The $U(1)_Y$ -hyper charge of the Higgs doublet is $Y_H = 1/2$. We define the SM Yukawa couplings of quarks as in [6],

$$-\mathcal{L}_{\text{Yuk}} = \bar{q}_L Y_d H d_R + \bar{q}_L Y_u \tilde{H} u_R + \text{h.c.} . \quad (82)$$

The Higgs doublet H is parameterized in R_ξ -gauge as

$$H = \begin{pmatrix} H^+ \\ H^0 \end{pmatrix} = \begin{pmatrix} G^+ \\ (v + h^0 + iG^0)/\sqrt{2} \end{pmatrix}, \quad (83)$$

with G^+ and G^0 denoting the would-be-Goldstone bosons and h^0 the SM Higgs. In the absence of dim-6 effects $v = (\sqrt{2}G_F)^{-1/2}$, however, in SMEFT this equality is not guaranteed anymore and changed by the dim-6 contribution of the H^6 -operator [17] that modifies the Higgs potential.

The derivatives in $\psi^2 H^2 D$ operators (3) and (4) are defined in a Hermitian way [6],

$$\begin{aligned} H^\dagger i \overleftrightarrow{\mathcal{D}}_\mu H &\equiv i [H^\dagger (\mathcal{D}_\mu H) - (\mathcal{D}_\mu H)^\dagger H], \\ H^\dagger i \overleftrightarrow{\mathcal{D}}_\mu^a H &\equiv i [H^\dagger \sigma^a (\mathcal{D}_\mu H) - (\mathcal{D}_\mu H)^\dagger \sigma^a H]. \end{aligned} \quad (84)$$

After EWSB the $\psi^2 H^2 D$ operators take rather lengthy forms in the mass eigenbasis:

$$[\mathcal{C}_{Hd}]_{ij} [\mathcal{O}_{Hd}]_{ij} = [\mathcal{C}_{Hd}]_{ij} (H^\dagger i \overleftrightarrow{\mathcal{D}}_\mu H) [\bar{d}^i \gamma^\mu P_R d^j], \quad (85)$$

$$[\mathcal{C}_{Hq}^{(1)}]_{ij} [\mathcal{O}_{Hq}^{(1)}]_{ij} = [\mathcal{C}_{Hq}^{(1)}]_{ij} (H^\dagger i \overleftrightarrow{\mathcal{D}}_\mu H) (V_{mi} V_{nj}^* [\bar{u}^m \gamma^\mu P_L u^n] + [\bar{d}^i \gamma^\mu P_L d^j]), \quad (86)$$

$$\begin{aligned} [\mathcal{C}_{Hq}^{(3)}]_{ij} [\mathcal{O}_{Hq}^{(3)}]_{ij} &= \left([\mathcal{C}_{Hq}^{(3)}]_{ij} (H^\dagger i \overleftrightarrow{\mathcal{D}}_\mu^1 H - i H^\dagger i \overleftrightarrow{\mathcal{D}}_\mu^2 H) V_{mi} [\bar{u}^m \gamma^\mu P_L d^j] + \text{h.c.} \right) \\ &+ [\mathcal{C}_{Hq}^{(3)}]_{ij} (H^\dagger i \overleftrightarrow{\mathcal{D}}_\mu^3 H) (V_{mi} V_{nj}^* [\bar{u}^m \gamma^\mu P_L u^n] - [\bar{d}^i \gamma^\mu P_L d^j]). \end{aligned} \quad (87)$$

Note that CKM elements appear in the mass eigenbasis only whenever left-handed up-type quarks are involved, due to the choice explained in Section 2.1. The terms with covariant derivatives contain gauge, Higgs and would-be-Goldstone interactions that are equal in \mathcal{O}_{Hd} and the singlet-operator $\mathcal{O}_{Hq}^{(1)}$,

$$\begin{aligned} H^\dagger i \overleftrightarrow{\mathcal{D}}_\mu H &= -(v + h^0)(\partial_\mu G^0) + G^0(\partial_\mu h^0) + iG^- \overleftrightarrow{\partial}_\mu G^+ \\ &+ g_2 [(v + h^0 - iG^0) G^+ W_\mu^- + \text{h.c.}] + 2eG^- G^+ A_\mu \\ &+ \frac{g_Z}{2} [2(c_W^2 - s_W^2)G^- G^+ - v^2 - 2vh^0 - (h^0)^2 - (G^0)^2] Z_\mu, \end{aligned} \quad (88)$$

but differ for the triplet operator $\mathcal{O}_{Hq}^{(3)}$,

$$\begin{aligned} H^\dagger i \overleftrightarrow{\mathcal{D}}_\mu^3 H &= +(v + h^0)(\partial_\mu G^0) - G^0(\partial_\mu h^0) + iG^- \overleftrightarrow{\partial}_\mu G^+ + 2eG^- G^+ A_\mu \\ &+ \frac{g_Z}{2} [2(c_W^2 - s_W^2)G^- G^+ + v^2 + 2vh^0 + (h^0)^2 + (G^0)^2] Z_\mu, \end{aligned} \quad (89)$$

$$\begin{aligned} \frac{1}{\sqrt{2}}(H^\dagger i \overleftrightarrow{\mathcal{D}}_\mu^1 H - iH^\dagger i \overleftrightarrow{\mathcal{D}}_\mu^2 H) &= vi\partial_\mu G^+ + h^0 i \overleftrightarrow{\partial}_\mu G^+ + G^0 \overleftrightarrow{\partial}_\mu G^+ \\ &+ \frac{g_2}{2} [v^2 + 2vh^0 + (h^0)^2 + (G^0)^2 + 2G^- G^+] W_\mu^+ \\ &+ (v + h^0 - iG^0)G^+ [eA_\mu - g_Z s_W^2 Z_\mu]. \end{aligned} \quad (90)$$

Here $g_Z \equiv \sqrt{g_1^2 + g_2^2}$, $s_W \equiv \sin \theta_W$ and $c_W \equiv \cos \theta_W$, where θ_W denotes the weak mixing angle, which again differs by dim-6 contributions from its SM analogue. The partial derivatives act only on fields within parentheses. Eventually only a few terms are required for the Feynman rules that enter the calculation of the diagrams in Fig. 1.

The $\psi^2 H^2 D$ operators (3)-(5) undergo also mixing among themselves. Here we list for completeness the Yukawa-enhanced contributions [12]:

$$\begin{aligned} \dot{\mathcal{C}}_{Hq}^{(1)} &= 6 \text{Tr}[Y_u Y_u^\dagger] \mathcal{C}_{Hq}^{(1)} + 2 \left(Y_u Y_u^\dagger \mathcal{C}_{Hq}^{(1)} + \mathcal{C}_{Hq}^{(1)} Y_u Y_u^\dagger \right), \\ &- \frac{9}{2} \left(Y_u Y_u^\dagger \mathcal{C}_{Hq}^{(3)} + \mathcal{C}_{Hq}^{(3)} Y_u Y_u^\dagger \right) - Y_u \mathcal{C}_{Hu} Y_u^\dagger, \\ \dot{\mathcal{C}}_{Hq}^{(3)} &= 6 \text{Tr}[Y_u Y_u^\dagger] \mathcal{C}_{Hq}^{(3)} + Y_u Y_u^\dagger \mathcal{C}_{Hq}^{(3)} + \mathcal{C}_{Hq}^{(3)} Y_u Y_u^\dagger - \frac{3}{2} \left(Y_u Y_u^\dagger \mathcal{C}_{Hq}^{(1)} + \mathcal{C}_{Hq}^{(1)} Y_u Y_u^\dagger \right), \\ \dot{\mathcal{C}}_{Hu} &= -2Y_u^\dagger \mathcal{C}_{Hq}^{(1)} Y_u + 6 \text{Tr}[Y_u Y_u^\dagger] \mathcal{C}_{Hu} + 4 \left(Y_u^\dagger Y_u \mathcal{C}_{Hu} + \mathcal{C}_{Hu} Y_u^\dagger Y_u \right), \\ \dot{\mathcal{C}}_{Hd} &= 6 \text{Tr}[Y_u Y_u^\dagger] \mathcal{C}_{Hd}, \\ \dot{\mathcal{C}}_{Hud} &= 6 \text{Tr}[Y_u Y_u^\dagger] \mathcal{C}_{Hud} + 3Y_u^\dagger Y_u \mathcal{C}_{Hud}. \end{aligned} \quad (91)$$

These ADMs show that in SMEFT the LH-Z interactions $\mathcal{C}_{Hq}^{(1,3)}$ do not generate RH-Z interactions in the down-type sector (\mathcal{C}_{Hd}) and vice versa. However, there *is* mixing of

the LH- Z interaction $\mathcal{C}_{Hq}^{(1)}$ into the RH- Z interactions of up-type sector (\mathcal{C}_{Hu}) and vice versa. In order to draw conclusions on the phenomenological impact, the explicit flavour structure should be worked out though, see for example (28). In the main part of our work we assume a scenario where $\psi^2 H^2 D$ operators are the dominant ones at μ_Λ and generate $\Delta F = 2$ - ψ^4 operators at μ_{ew} . For this purpose we have neglected the mixing among the various $\psi^2 H^2 D$ operators in the evolution from μ_Λ to μ_{ew} in (23), which enters loop-suppressed in $\Delta F = 2$ processes.

References

- [1] S. L. Glashow, J. Iliopoulos and L. Maiani, *Weak Interactions with Lepton-Hadron Symmetry*, *Phys. Rev.* **D2** (1970) 1285–1292.
- [2] T. Inami and C. Lim, *Effects of Superheavy Quarks and Leptons in Low-Energy Weak Processes* $K_L \rightarrow \mu^+ \mu^-$, $K^+ \rightarrow \pi^+ \nu \bar{\nu}$ and $K^0 - \bar{K}^0$, *Prog. Theor. Phys.* **65** (1981) 297.
- [3] G. Buchalla, A. J. Buras and M. K. Harlander, *Penguin box expansion: Flavor changing neutral current processes and a heavy top quark*, *Nucl. Phys.* **B349** (1991) 1–47.
- [4] A. J. Buras and J. Girrbach, *Towards the Identification of New Physics through Quark Flavour Violating Processes*, *Rept. Prog. Phys.* **77** (2014) 086201, [1306.3775].
- [5] W. Buchmüller and D. Wyler, *Effective Lagrangian Analysis of New Interactions and Flavor Conservation*, *Nucl. Phys.* **B268** (1986) 621–653.
- [6] B. Grzadkowski, M. Iskrzynski, M. Misiak and J. Rosiek, *Dimension-Six Terms in the Standard Model Lagrangian*, *JHEP* **1010** (2010) 085, [1008.4884].
- [7] C. Arzt, M. B. Einhorn and J. Wudka, *Patterns of deviation from the standard model*, *Nucl. Phys.* **B433** (1995) 41–66, [hep-ph/9405214].
- [8] A. J. Buras, F. De Fazio and J. Girrbach, *The Anatomy of Z' and Z with Flavour Changing Neutral Currents in the Flavour Precision Era*, *JHEP* **1302** (2013) 116, [1211.1896].
- [9] A. J. Buras, D. Buttazzo and R. Knegjens, *$K \rightarrow \pi \nu \bar{\nu}$ and ϵ'/ϵ in Simplified New Physics Models*, *JHEP* **11** (2015) 166, [1507.08672].
- [10] A. J. Buras, *New physics patterns in ϵ'/ϵ and ϵ_K with implications for rare kaon decays and ΔM_K* , *JHEP* **04** (2016) 071, [1601.00005].
- [11] M. Endo, T. Kitahara, S. Mishima and K. Yamamoto, *Revisiting Kaon Physics in General Z Scenario*, *Phys. Lett.* **B771** (2017) 37–44, [1612.08839].

- [12] E. E. Jenkins, A. V. Manohar and M. Trott, *Renormalization Group Evolution of the Standard Model Dimension Six Operators II: Yukawa Dependence*, *JHEP* **01** (2014) 035, [1310.4838].
- [13] K. Ishiwata, Z. Ligeti and M. B. Wise, *New Vector-Like Fermions and Flavor Physics*, *JHEP* **10** (2015) 027, [1506.03484].
- [14] C. Bobeth, A. J. Buras, A. Celis and M. Jung, *Patterns of Flavour Violation in Models with Vector-Like Quarks*, *JHEP* **04** (2017) 079, [1609.04783].
- [15] F. del Aguila, M. Perez-Victoria and J. Santiago, *Observable contributions of new exotic quarks to quark mixing*, *JHEP* **0009** (2000) 011, [hep-ph/0007316].
- [16] E. E. Jenkins, A. V. Manohar and M. Trott, *Renormalization Group Evolution of the Standard Model Dimension Six Operators I: Formalism and λ Dependence*, *JHEP* **10** (2013) 087, [1308.2627].
- [17] R. Alonso, E. E. Jenkins, A. V. Manohar and M. Trott, *Renormalization Group Evolution of the Standard Model Dimension Six Operators III: Gauge Coupling Dependence and Phenomenology*, *JHEP* **04** (2014) 159, [1312.2014].
- [18] G. Buchalla, A. J. Buras and M. E. Lautenbacher, *Weak decays beyond leading logarithms*, *Rev. Mod. Phys.* **68** (1996) 1125–1144, [hep-ph/9512380].
- [19] J. Aebischer, A. Crivellin, M. Fael and C. Greub, *Matching of gauge invariant dimension-six operators for $b \rightarrow s$ and $b \rightarrow c$ transitions*, *JHEP* **05** (2016) 037, [1512.02830].
- [20] M. Ciuchini, E. Franco, V. Lubicz, G. Martinelli, I. Scimemi et al., *Next-to-leading order QCD corrections to $\Delta F = 2$ effective Hamiltonians*, *Nucl. Phys.* **B523** (1998) 501–525, [hep-ph/9711402].
- [21] A. J. Buras, M. Misiak and J. Urban, *Two loop QCD anomalous dimensions of flavor changing four quark operators within and beyond the standard model*, *Nucl. Phys.* **B586** (2000) 397–426, [hep-ph/0005183].
- [22] G. M. Pruna and A. Signer, *The $\mu \rightarrow e\gamma$ decay in a systematic effective field theory approach with dimension 6 operators*, *JHEP* **10** (2014) 014, [1408.3565].
- [23] R. Gauld, B. D. Pecjak and D. J. Scott, *One-loop corrections to $h \rightarrow b\bar{b}$ and $h \rightarrow \tau\bar{\tau}$ decays in the Standard Model Dimension-6 EFT: four-fermion operators and the large- m_t limit*, *JHEP* **05** (2016) 080, [1512.02508].
- [24] C. Bobeth and U. Haisch, *Anomalous triple gauge couplings from B -meson and kaon observables*, *JHEP* **09** (2015) 018, [1503.04829].
- [25] S. Alioli, V. Cirigliano, W. Dekens, J. de Vries and E. Mereghetti, *Right-handed charged currents in the era of the Large Hadron Collider*, *JHEP* **05** (2017) 086, [1703.04751].

- [26] C. Bobeth, M. Misiak and J. Urban, *Photonic penguins at two loops and m_t -dependence of $Br(B \rightarrow X_s \ell^+ \ell^-)$* , *Nucl. Phys.* **B574** (2000) 291–330, [[hep-ph/9910220](#)].
- [27] F. Feruglio, P. Paradisi and A. Pattori, *Revisiting Lepton Flavor Universality in B Decays*, *Phys. Rev. Lett.* **118** (2017) 011801, [[1606.00524](#)].
- [28] V. Cirigliano, W. Dekens, J. de Vries and E. Mereghetti, *An ϵ' improvement from right-handed currents*, *Phys. Lett.* **B767** (2017) 1–9, [[1612.03914](#)].
- [29] LHCb collaboration, R. Aaij et al., *Measurement of the $B_s^0 \rightarrow \mu^+ \mu^-$ branching fraction and effective lifetime and search for $B^0 \rightarrow \mu^+ \mu^-$ decays*, *Phys. Rev. Lett.* **118** (2017) 191801, [[1703.05747](#)].
- [30] W. Altmannshofer, C. Niehoff and D. M. Straub, *$B_s \rightarrow \mu^+ \mu^-$ as current and future probe of new physics*, *JHEP* **05** (2017) 076, [[1702.05498](#)].
- [31] RBC/UKQCD collaboration, N. Garron, R. J. Hudspith and A. T. Lytle, *Neutral Kaon Mixing Beyond the Standard Model with $n_f = 2 + 1$ Chiral Fermions Part 1: Bare Matrix Elements and Physical Results*, *JHEP* **11** (2016) 001, [[1609.03334](#)].
- [32] FERMILAB LATTICE, MILC collaboration, A. Bazavov et al., *$B_{(s)}^0$ -mixing matrix elements from lattice QCD for the Standard Model and beyond*, *Phys. Rev.* **D93** (2016) 113016, [[1602.03560](#)].
- [33] A. J. Buras, S. Jäger and J. Urban, *Master formulae for $\Delta F = 2$ NLO QCD factors in the standard model and beyond*, *Nucl. Phys.* **B605** (2001) 600–624, [[hep-ph/0102316](#)].
- [34] A. J. Buras, M. Jamin and P. H. Weisz, *Leading and next-to-leading QCD corrections to ϵ parameter and $B^0 - \bar{B}^0$ mixing in the presence of a heavy top quark*, *Nucl. Phys.* **B347** (1990) 491–536.
- [35] J. Brod and M. Gorbahn, *ϵ_K at Next-to-Next-to-Leading Order: The Charm-Top-Quark Contribution*, *Phys. Rev.* **D82** (2010) 094026, [[1007.0684](#)].
- [36] J. Brod and M. Gorbahn, *Next-to-Next-to-Leading-Order Charm-Quark Contribution to the CP Violation Parameter ϵ_K and ΔM_K* , *Phys. Rev. Lett.* **108** (2012) 121801, [[1108.2036](#)].
- [37] M. Jung, *Determining weak phases from $B \rightarrow J/\psi P$ decays*, *Phys. Rev.* **D86** (2012) 053008, [[1206.2050](#)].
- [38] K. De Bruyn and R. Fleischer, *A Roadmap to Control Penguin Effects in $B_d^0 \rightarrow J/\psi K_S^0$ and $B_s^0 \rightarrow J/\psi \phi$* , *JHEP* **03** (2015) 145, [[1412.6834](#)].
- [39] P. Frings, U. Nierste and M. Wiebusch, *Penguin contributions to CP phases in $B_{d,s}$ decays to charmonium*, *Phys. Rev. Lett.* **115** (2015) 061802, [[1503.00859](#)].

- [40] Z. Ligeti and D. J. Robinson, *Towards more precise determinations of the quark mixing phase β* , *Phys. Rev. Lett.* **115** (2015) 251801, [1507.06671].
- [41] R. Alonso, B. Grinstein and J. Martin Camalich, *$SU(2) \times U(1)$ gauge invariance and the shape of new physics in rare B decays*, *Phys. Rev. Lett.* **113** (2014) 241802, [1407.7044].
- [42] A. J. Buras, J. Girrbach-Noe, C. Niehoff and D. M. Straub, *$B \rightarrow K^{(*)}\nu\bar{\nu}$ decays in the Standard Model and beyond*, *JHEP* **1502** (2015) 184, [1409.4557].
- [43] NA48 collaboration, J. Batley et al., *A Precision measurement of direct CP violation in the decay of neutral kaons into two pions*, *Phys. Lett.* **B544** (2002) 97–112, [hep-ex/0208009].
- [44] KTeV collaboration, A. Alavi-Harati et al., *Measurements of direct CP violation, CPT symmetry, and other parameters in the neutral kaon system*, *Phys. Rev.* **D67** (2003) 012005, [hep-ex/0208007].
- [45] KTeV collaboration, E. Abouzaid et al., *Precise Measurements of Direct CP Violation, CPT Symmetry, and Other Parameters in the Neutral Kaon System*, *Phys. Rev.* **D83** (2011) 092001, [1011.0127].
- [46] T. Blum et al., *$K \rightarrow \pi\pi$ $\Delta I = 3/2$ decay amplitude in the continuum limit*, *Phys. Rev.* **D91** (2015) 074502, [1502.00263].
- [47] RBC, UKQCD collaboration, Z. Bai et al., *Standard Model Prediction for Direct CP Violation in K Decay*, *Phys. Rev. Lett.* **115** (2015) 212001, [1505.07863].
- [48] A. J. Buras, M. Gorbahn, S. Jäger and M. Jamin, *Improved anatomy of ϵ'/ϵ in the Standard Model*, *JHEP* **11** (2015) 202, [1507.06345].
- [49] A. J. Buras and J.-M. Gérard, *Upper Bounds on ϵ'/ϵ Parameters $B_6^{(1/2)}$ and $B_8^{(3/2)}$ from Large N QCD and other News*, *JHEP* **12** (2015) 008, [1507.06326].
- [50] A. J. Buras and J.-M. Gérard, *Final state interactions in $K \rightarrow \pi\pi$ decays: $\Delta I = 1/2$ rule vs. ϵ'/ϵ* , *Eur. Phys. J.* **C77** (2017) 10, [1603.05686].
- [51] T. Kitahara, U. Nierste and P. Tremper, *Singularity-free next-to-leading order $\Delta S = 1$ renormalization group evolution and ϵ'_K/ϵ_K in the Standard Model and beyond*, *JHEP* **12** (2016) 078, [1607.06727].
- [52] G. Isidori and R. Unterdorfer, *On the short-distance constraints from $K_{L,S} \rightarrow \mu^+\mu^-$* , *JHEP* **01** (2004) 009, [hep-ph/0311084].
- [53] G. D'Ambrosio, G. Isidori and J. Portoles, *Can we extract short-distance information from $Br(K_L \rightarrow \mu^+\mu^-)$?*, *Phys. Lett.* **B423** (1998) 385–394, [hep-ph/9708326].
- [54] M. Blanke, A. J. Buras and S. Recksiegel, *Quark flavour observables in the Littlest Higgs model with T -parity after LHC Run 1*, *Eur. Phys. J.* **C76** (2016) 182, [1507.06316].